

AD-A224 074

NAVAL POSTGRADUATE SCHOOL

Monterey, California



THESIS

DTIC
ELECTE
JUL 19 1990
S E D

AN EXPERIMENTAL INVESTIGATION
OF STRAND BURNING
METALLIZED SOLID PROPELLANTS

by

Kevin J. Arnold

December, 1989

Thesis Advisor:

D. W. Netzer

Approved for public release; distribution
is unlimited.

REPORT DOCUMENTATION PAGE

1a. REPORT SECURITY CLASSIFICATION UNCLASSIFIED			1b. RESTRICTIVE MARKINGS		
2a. SECURITY CLASSIFICATION AUTHORITY			3. DISTRIBUTION/AVAILABILITY OF REPORT Approved for public release; distribution is unlimited.		
2b. DECLASSIFICATION/DOWNGRADING SCHEDULE					
4. PERFORMING ORGANIZATION REPORT NUMBER(S)			5. MONITORING ORGANIZATION REPORT NUMBER(S)		
6a. NAME OF PERFORMING ORGANIZATION Naval Postgraduate School		6b. OFFICE SYMBOL (If applicable) Code 67		7a. NAME OF MONITORING ORGANIZATION Naval Postgraduate School	
6c. ADDRESS (City, State, and ZIP Code) Monterey, California 93943-5000			7b. ADDRESS (City, State, and ZIP Code) Monterey, California 93943-5000		
8a. NAME OF FUNDING/SPONSORING ORGANIZATION Air Force Astronautics Laboratory		8b. OFFICE SYMBOL (If applicable)		9. PROCUREMENT INSTRUMENT IDENTIFICATION NUMBER	
8c. ADDRESS (City, State, and ZIP Code) Edwards Air Force Base California			10. SOURCE OF FUNDING NUMBERS		
			PROGRAM ELEMENT NO.	PROJECT NO.	TASK NO.
			WORK UNIT ACCESSION NO.		
11. TITLE (Include Security Classification) AN EXPERIMENTAL INVESTIGATION OF STRAND BURNING METALLIZED SOLID PROPELLANTS					
12. PERSONAL AUTHOR(S) Arnold, Kevin J.					
13a. TYPE OF REPORT Master's Thesis		13b. TIME COVERED FROM _____ TO _____		14. DATE OF REPORT (Year, Month, Day) 1989, December	
15. PAGE COUNT 74					
16. SUPPLEMENTARY NOTATION The views expressed in this thesis are those of the author and do not reflect the official policy or position of the Department of Defense or the					
17. U.S. Government:			18. SUBJECT TERMS (Continue on reverse if necessary and identify by block number)		
FIELD	GROUP	SUB-GROUP	Solid Propellants		
			Combustion Bomb		
			Particle Sizes		
19. ABSTRACT (Continue on reverse if necessary and identify by block number) Characteristics of the products of combustion of metallized solid propellant strands at pressures between 250 and 750 psi were investigated using holography and light scattering measurements. In addition, scanning electron microscope and light scattering measurements were used to examine quenched residue. A reduced smoke ZrC propellant and three propellants of varying aluminum loading (2%, 4.8%, and 16%) were examined. The objective of the experiments was to provide sufficient particle data from strand burners to make it possible to determine if any correlation of results from this method of analysis could be made with results from other more complex solid propellant motor measurements, such as plume probe and signature measurements. The results of these efforts reflected the inability of any single technique of analysis to completely describe particle size distributions. These results also suggest the need for modification of current experimental apparatus and procedures. <i>25/</i>					
20. DISTRIBUTION/AVAILABILITY OF ABSTRACT <input checked="" type="checkbox"/> UNCLASSIFIED/UNLIMITED <input type="checkbox"/> SAME AS RPT. <input type="checkbox"/> DTIC USERS			21. ABSTRACT SECURITY CLASSIFICATION Unclassified		
22a. NAME OF RESPONSIBLE INDIVIDUAL Prof. D. W. Netzer			22b. TELEPHONE (Include Area Code) (408) 646-2980		22c. OFFICE SYMBOL Code 67 Nt

Approved for public release; distribution is unlimited.

An Experimental Investigation
of Strand Burning
Metallized Solid Propellants

by

Kevin J. Arnold
Captain, United States Army
B.S., United States Military Academy

Submitted in partial fulfillment
of the requirements for the degree of

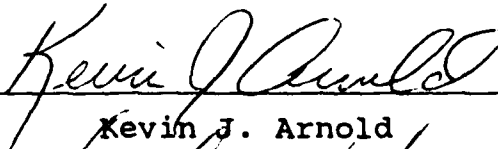
MASTER OF SCIENCE IN ENGINEERING SCIENCE

from the

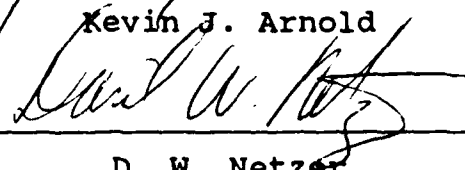
NAVAL POSTGRADUATE SCHOOL

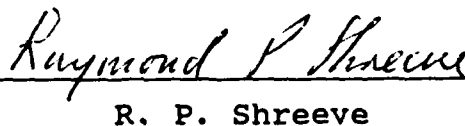
December 1989


Author:


Kevin J. Arnold

Approved by:


D. W. Netzer


R. P. Shreeve



E. R. Wood, Chairman
Department of Aeronautics and Astronautics

ABSTRACT

Characteristics of the products of combustion of metalized solid propellant strands at pressures between 250 and 750 psi were investigated using holography and light scattering measurements. In addition, scanning electron microscope and light scattering measurements were used to examine quenched residue. A reduced smoke ZrC propellant and three propellants of varying aluminum loading (2%, 4.8%, and 16%) were examined. The objective of the experiments was to provide sufficient particle data from strand burners to make it possible to determine if any correlation of results from this method of analysis could be made with results from other more complex solid propellant motor measurements, such as plume probe and signature measurements. The results of these efforts reflected the inability of any single technique of analysis to completely describe particle size distributions. These results also suggest the need for modification of current experimental apparatus and procedures.



iii

Accession For	
NTIS GRA&I	<input checked="checked" type="checkbox"/>
DTIC TAB	<input type="checkbox"/>
Unannounced	<input type="checkbox"/>
Justification	
By _____	
Distribution/	
Availability Codes	
Dist	Avail and/or Special
A-1	

TABLE OF CONTENTS

I.	INTRODUCTION-----	1
II.	EXPERIMENTAL APPARATUS-----	4
III.	EXPERIMENTAL PROCEDURES-----	11
	A. COMBUSTION BOMB AND HOLOGRAPHY-----	11
	B. COMBUSTION BOMB AND MASTERSIZER-----	14
	C. RESIDUE COLLECTION-----	15
	D. RESIDUE PARTICLE SIZING-----	16
	E. SEM SAMPLE PREPARATION AND MICROSCOPY-----	18
	F. BURN RATE DETERMINATION-----	19
IV.	RESULTS AND DISCUSSION-----	20
	A. COMBUSTION BOMB AND HOLOGRAPHY-----	20
	B. COMBUSTION BOMB AND MASTERSIZER-----	21
	C. RESIDUE COLLECTION-----	23
	D. SEM RESIDUE RESULTS-----	24
	E. MASTERSIZER RESIDUE PARTICLE SIZING RESULTS---	25
	F. BURN RATE DETERMINATION-----	26
V.	CONCLUSIONS AND RECOMMENDATIONS-----	27
	APPENDIX A - MASTERSIZER VALIDATION-----	30
	LIST OF REFERENCES-----	62
	INITIAL DISTRIBUTION LIST-----	63

LIST OF TABLES

1. Propellant Composition-----	34
2. D ₃₂ Data Summary-----	35
3. D ₄₃ Data Summary-----	36
4. Burn Rate Data (r; in/sec)-----	37

LIST OF FIGURES

1.	Holography Combustion Bomb Schematic-----	38
2.	Holography Combustion Bomb-----	39
3.	Holography Ignition Setup-----	39
4.	Holocamera Schematic-----	40
5.	Laser, Holocamera and Combustion Bomb-----	40
6.	Holocamera Reconstruction Setup-----	41
7.	Combustion Bomb with Mastersizer-----	41
8.	Collection Combustion Bomb Schematic-----	42
9.	Collection Combustion Bomb-----	43
10.	Collection Ignition Setup-----	43
11.	Remote Control Panels-----	44
12.	Residue Collection Setup-----	44
13a.	Hologram of DD5 (x1 magnification)-----	45
13b.	Hologram of DD5 (x4 magnification)-----	45
13c.	Hologram of DDSS (x1 magnification)-----	46
14a.	SEM of DD1 at 100 psi-----	47
14b.	SEM of DD1 at 250 psi-----	47
14c.	SEM of DD1 at 500 psi-----	48
14d.	SEM of DD1 at 750 psi-----	48
14e.	SEM of DD5 at 100 psi-----	49
14f.	SEM of DD5 at 250 psi-----	49
14g.	SEM of DD5 at 500 psi-----	50
14h.	SEM of DD5 at 750 psi-----	50
14i.	SEM of DDSS at 250 psi-----	51

14j.	SEM of DDSS at 500 psi-----	51
14k.	SEM of ZrC at 100 psi-----	52
14l.	SEM of ZrC at 250 psi-----	52
14m.	SEM of ZrC at 500 psi-----	53
14n.	SEM of ZrC at 750 psi-----	53
15a.	Collection and SEM Numerical Comparison: DD1 at 500 psi-----	54
15b.	Collection and SEM Numerical Comparison: DD5 at 500 psi-----	54
15c.	Collection and SEM Numerical Comparison: DDSS at 500 psi-----	55
15d.	Collection and SEM Numerical Comparison: ZrC at 500 psi-----	55
16a.	Mastersizer Results of Collected DD1 at 500 psi---	56
16b.	Mastersizer Plots of Collected DD1 at 500 psi----	56
16c.	Mastersizer Results of Collected DD5 at 500 psi---	57
16d.	Mastersizer Plots of Collected DD5 at 500 psi----	57
16e.	Mastersizer Results of Collected DDSS at 500 psi--	58
16f.	Mastersizer Plots of Collected DDSS at 500 psi----	58
16g.	Mastersizer Results of Collected ZrC at 500 psi---	59
16h.	Mastersizer Plots of Collected ZrC at 500 psi----	59
17a.	Mastersizer Validation Results: 0.5 micron spheres-----	60
17b.	Mastersizer Validation Plots: 0.5 micron spheres-----	60
17c.	Mastersizer Validation Individual and Mixed Samples-----	61
17d.	Mastersizer Validation Individual and Mixed Samples-----	61

LIST OF SYMBOLS

a	Coefficient in Equation (1)
d	Particle Diameter
D_{32}	<u>Sarter Mean Diameter</u> = $\Sigma nd^3 / \Sigma nd^2$
D_{43}	$\Sigma nd^4 / \Sigma nd^3$
DD_	Propellant Designations (Table 1)
n	Exponent in Equation (1)
N	Numbers of Particles with Diameter d
p	Pressure in psia
r	Burning Rate in ins/sec
SEM	Scanning Electron Microscope

ACKNOWLEDGMENTS

Whenever the concept of thesis work originated, its inventor must have had this type of thesis experience in mind. Working for and with Professor Dave Netzer has been both educational and enjoyable. I am particularly appreciative of his patience and sense of humor. I am similarly grateful to Harry Conner, whose technical expertise was invaluable and whose personality has been fundamental to a working atmosphere of encouragement and accomplishment. I would also like to thank the Aeronautical Engineering technical staff for their assistance in making the necessary apparatus. Finally, thanks to my full-time partner and wife, Tami, for her never-ending understanding and support.

I. INTRODUCTION

The role of solid propellant rocket motors in the modern military strategies of countries around the world continues to expand. The introduction of metal particles in solid propellants is done primarily for the increased specific impulse, I_{sp} , which these higher energy fuels provide. Metal particles can also produce potentially positive influences in the areas of pressure oscillation suppression and reduced sensitivity of motor operating pressure to propellant temperature (a in the burning rate expression $r=ap^n$). Possible disadvantages of metallized fuels include, but are not limited to: decreased specific impulse efficiency due to thermal and velocity lags of particles in the exhaust nozzle flow (two-phase flow losses) as well as to incomplete combustion within the combustor; undesirable plume signature characteristics; and an overall lack of understanding (and subsequent difficulty for accurate modeling) introduced by the quite complex history of metallic particles from their as-cast condition in the propellant to their characteristics in the exhaust plume.

There are, in general, two types of metallized fuel combustion. In cases where the melting point temperature of the oxide is greater than the melting point temperature of the pure metal (such as for the most commonly used additive,

aluminum (Al)), a vapor phase combustion occurs similar to that for liquid fuels. The resulting gaseous diffusion flame is frequently characterized as "detached." The second condition (commonly called a "surface" flame) results when the metal, such as zirconium carbide, has a melting point temperature greater than that of its oxide [Ref. 1]. In both cases, it should be noted, some level of surface agglomeration can take place, resulting in exhausted particles capable of containing large numbers of the original particles.

While a wide range of experimental techniques are available for pursuing a better understanding of metallized solid fuel particulate behavior, the scope of this investigation was limited to a thorough examination of combustion bomb tests of propellant strands. The specific propellants used contained 2.00%, or 4.68% aluminum (provided by the Air Force Astronautics Laboratory (AFAL), Edwards, California), 16% aluminum (provided by Morton Thiokol), or 1.00% zirconium carbide (provided by Naval Weapons Center, China Lake, California). Table I includes detailed propellant composition data. The objective of these experiments was to provide sufficient particle data to make it possible to determine if any correlation of strand burning data could be made with the results from other more complex solid propellant motor measurements of interest, such as plume particulate characteristics and signature measurements [Ref. 2].

A combination of tools, including two combustion bombs, were used in collecting the desired strand-burning particle data. One combustion bomb made it possible to quench and collect propellant residues. After cleaning, these particles could then be examined using both a Malvern Mastersizer particle sizer and a scanning electron microscope (SEM). SEM pictures provide the additional possibility for automated data processing (ADP) to obtain the particle size distribution. The second combustion bomb was designed to operate within the confines of a holocamera, providing a high-resolution visual record of particle behavior during the strand burn. This second bomb could also be operated in the field of view of the Mastersizer, providing comparable high-resolution particle data during the strand burn.

II. EXPERIMENTAL APPARATUS

The combustion bomb used in the holographic investigations was constructed of two pieces of 304 stainless steel with a core volume of only 25 cubic inches and an inside diameter of 1.7 inches. The bomb had two parallel windows, each 1.5 inches in diameter with a usable diameter of approximately 1.25 inches. O-ring seals were used with each of the windows and at the junction of the two pieces of the combustion bomb. Figure 1 is a schematic of the combustion bomb. Figure 2 is a photograph of the combustion bomb. The maximum operating pressure of the combustion bomb was 1000 psi and the maximum pressure used in this investigation was 750 psi. The propellant strand ignition system consisted of two upright copper electrodes and a centered hollow stainless steel tube, with a set screw providing height adjustment of the pedestal holding the propellant strand. The ignition lead wires were run from a 12 volt battery through a Conax adapter positioned on the bomb such that the inlet to the core was between the lower and upper diffusion plates. Ignition was triggered by a switch and the burn was initiated by .008 inch diameter nickel - chromium wire strung and soldered between two stripped copper wires, which were then inserted into the two electrodes. Figure 3 is a photograph of the ignition system.

A TRW Q-switched pulsed ruby laser was used for the holographic investigation. The laser output was expanded and collimated to a maximum diameter of 1.26 inches. All laser optics were located in one chest with a dark field autocollimator and a helium-neon laser for alignment. Cooling was provided by a separate cabinet containing coolant and a refrigeration system. Laser output was 1 joule in a 50 nanosecond pulse of 0.6943 micron wavelength light [Ref. 2].

The holocamera, also built by TRW, Inc., was used to split the laser light into two beams. Using one as the reference beam and passing the other, the scene beam, through the windows of the combustion bomb during combustion allowed a hologram to be obtained by the interference pattern formed by recombination of the two beams on the plate. The holographic plates were 4 X 5 inch Afga-Gevaert 8E75 HD glass recording plates. A Uniblitz Model 225 electrical capping shutter was used inside the removable lens-plate holder. The shutter was connected to a control box which allowed for the opening of the shutters to coincide with the firing of the laser. The holocamera was equipped with an opaque diffuser in the scene beam path to eliminate the schlieren effects caused by the burning particles. In addition, an optical filter was contained in the lens-plate box to exclude flame light, but pass the laser light. The

holocamera is described in detail in Reference 3. Figure 4 is a schematic of the holocamera while Figure 5 is a photo of the laser, holocamera, and combustion bomb.

After the holographic plate was developed, it was returned to the removable lens-plate box and placed on a stand of an observation microscope. A Spectra Physics Model 165-11 Krypton-ion CW gas laser provided the rear illumination of the developed hologram. The laser had an output of 500 milliwatts at a wavelength of 0.6471 microns. The holographic plate was placed at an angle of approximately 60 degrees with the laser. The hologram was then reconstructed on a rotating mylar disc placed at the focal point of a variable power observation microscope. This process reduced speckle during reconstruction. Particle data was gathered from a high resolution monitor or directly through reticles in the microscope eyepiece. Photographs of the reconstruction scene were taken using either a 35 millimeter or Polaroid camera. Figure 6 is a photograph of the reconstruction setup.

Use of the same laser for both taking and reconstructing the hologram should yield the best resolution. The use of the pulsed ruby laser for taking holograms allowed for better penetration of the smoke generated by combustion in the bomb than the krypton-ion laser, and it provided the stop action required for the moving particles. However, the use of the continuous wave krypton-ion CW laser was required

for viewing the reconstructed holograms. The use of these two different lasers, with only small differences in wavelength, provided the best system for obtaining good quality holograms with only minor degradation in resolution.

The narrow combustion bomb also provided the ability to directly apply light scattering techniques to measure particle size distributions during the strand burn. A Malvern Mastersizer system was used to accomplish this. Figure 7 is a photograph of the Mastersizer mounted around the combustion bomb.

The combustion bomb used for the non-holographic investigations was constructed of two pieces of stainless steel with a core volume of 90 cubic inches and an inside diameter of 3.5 inches. The bomb had two large windows (2.4 inches in viewing diameter). O-ring seals were used with each of the windows and at the junction of the two pieces of the combustion bomb. Figure 8 is a schematic of the combustion bomb. Figure 9 is a photograph of the combustion bomb. The maximum operating pressure for the combustion bomb was 800 psi and the maximum pressure used in the investigation was 750 psi. The propellant strand ignition system consisted of two copper electrodes, with the propellant strand mounted between the electrodes. A 0.008 inch diameter nickel-chromium ignition wire was then strung between the electrodes to make contact with the top of the propellant strand. Figure 10 contains a photograph of the propellant

strand ignition setup. The ignition wires were tightened between the electrodes to insure contact between the ignition wire and the propellant strand and to ensure rapid and uniform ignition of the propellant surface. The ignition wire was connected in series with a variable resistor to control the current provided by a 12 volt DC wet cell battery. A continuity check could be made from the control booth to verify a complete circuit existed. The operating pressure in each of the combustion bombs was controlled using a dome loaded regulator located in the control booth. A gauge showing the bomb pressure was also located in the control booth. An actuator valve was pressurized to 100 psi and set to engage from the control booth to introduce a nitrogen flow into the bottom of the combustion bomb through a porous plate. The nitrogen flow was then exhausted through the top of the combustion bomb, through an exhaust line, and then to the outside atmosphere. This exhaust or purge flow rate was regulated manually by a valve located in the exhaust line.

Ignition of the propellant strand, pressurization of the combustion bomb and operation of the holocamera and laser were controlled from a panel located in a control booth for safety reasons. The booth provided viewing of the combustion bomb through a one inch thick Plexiglas window.

Figure 11 is a photograph of the remote control panels. These remote control panels provided controlled timing of ignition and laser operations.

Combustion residue was collected using a stainless steel collection cup designed and built for the bomb in which it was used. The cup had a one inch diameter and was 1.18 inches in depth. Distilled water was added to a depth of 0.50 inches in the collection cup to serve as a quenching and collection medium. The propellant strands were loaded upside down to fire directly into the fluid, with approximately 0.25 inches from the surface of the propellant strand to the surface of the fluid. The combustion bomb was then pressurized with nitrogen. Figure 12 is a photograph of the residue collection apparatus. The propellant ignition wire was run through small holes in the sides of the collection device, allowing the propellant strand to lie inverted on the wire and the strand pedestal to be secured.

Collected specimens were then transferred to beakers and ultrasonically cleaned using methanol as a bath. The particle residue was then examined using light diffraction techniques. The previously mentioned Malvern product, the Mastersizer, which employs reverse Fourier optics to achieve resolution down to 0.1 microns, was used. A description of procedures and results of efforts to validate the Mastersizer capability are included in Appendix A. Several drops of each sample were also allowed to dry onto pedestals

designed for use with a scanning electron microscope (SEM). A thin gold coating was applied with a Denton Vacuum Evaporator to insure the required conductivity. SEM observations were then made using both a Hitachi S-450 and a Stereoscan 200 made by Cambridge Instruments, Buffalo, New York. The photographs taken on both apparatus were made using Polaroid Type 52 film [Ref. 4].

III. EXPERIMENTAL PROCEDURES

A. COMBUSTION BOMB AND HOLOGRAPHY

The 4.68% and 16% aluminum propellants were each examined during burns at 500 psi. The propellant compositions are listed at Table I. The propellant strands were mounted onto stainless steel posts using wood glue, and sized to provide acceptable obscuration and particle presence. The 8 x 5 x 1.5 mm strand dimensions were selected to minimize the optical path length and maximize use of the window width. The nitrogen purge rate was increased to a level which prevented particles from impinging on the window surfaces. The propellant strand ignition system was set up as detailed in the Experimental Apparatus section. All operations were conducted from behind the control booth enclosure for maximum safety.

Initial calibration of the holographic system was accomplished using the pulsed ruby laser and the combustion bomb. Calibration targets were inserted to determine resolution. The bomb was windowed and a diffuser was used in the scene beam to match the system setup of the actual firing runs. The 0.75 inch thick windows had no appreciable affect on the optical path length of the scene beam. The scene beam

optical path length must match the reference beam path length to ensure maximum coherence and good resolution in the hologram.

A 1951 USAF resolution bar target was used for calibration. Resolution for the USAF target was approximately twelve microns. The diameter of the speckle in the holograms was approximately 5 - 8 microns and remained as the limiting factor in the resolution obtained.

Initial preparation of the system included proper setup and a thorough cleaning of the combustion bomb windows. The propellant was cut to predetermined dimensions in an effort to achieve the desired obscuration. The propellant and ignition wires were then mounted and the bomb properly sealed.

The laser and holocamera were then aligned using the Helium-Neon pointing laser. Cross hairs were used to spatially align the scene and reference beams. After final alignment, the cross hairs were removed, the diffuser was connected and the He-Ne laser turned off. The holocamera was then set up with a holographic plate, electronic shutter, and a narrow pass filter to eliminate the flame envelopes. The electronically operated shutter was connected to the control box, which was set to operate the shutter and fire the laser. The reference beam blocking plate in the

holocamera was then pulled open. Purge nitrogen was turned-on. The ruby laser was turned on and configured for either a ten or 50 nanosecond pulse.

The firing of the laser was carried out from the remote panels in the control booth. The internal pressure was set using the dome loader, also behind the control booth shield. When the set-up was ready, the laser capacitor bank charging control was turned on with a key and the nitrogen purge initiated. Because timing was not critical, the firing sequence was done manually. The opening of the shutter and firing of the laser was initiated immediately after ignition of the propellant strand.

Hologram developing was accomplished by removing the exposed holographic plate in a darkroom aided by a Kodak Safelight. The following steps were used in the process:

1. Immerse in Kodak HRP or D19 developer for approximately 10 second intervals until visual inspection under the Safelight showed a slight opacity.
2. Rinse in Kodak Stop Bath for 30 seconds to stop development.
3. Rinse in water for five seconds.
4. Immerse in Kodak Rapid Fix for five minutes to set the image.
5. Rinse in water for ten minutes.
6. Immerse in Kodak Photo-Flo solution for 30 seconds.
7. Allow to air dry for two to three hours before reconstructing hologram.

The holograms were reconstructed using the Krypton-Ion laser for rear illumination. The holographic plate was reinserted into the lens-plate box, which was placed onto a stand of an observation microscope. The beam and hologram plate were initially aligned with a 60 degree angle between them to pass the beam through the plate at the original scene beam angle. Then a decrease of approximately 9.5 degrees in the angle during reconstruction was used to compensate for the wavelength difference between the ruby and krypton lasers. Final tuning of the illumination beam angle was accomplished while observing a reconstructed image of a resolution target. The reconstructed hologram was then viewed, with the variable power microscope directly or by connecting a CCTV camera (Panasonic Model WV-1460) into the microscope and observing the picture on a monitor. A mylar disk connected to the microscope was used to help in focusing and, while rotating, served to blur the speckle, minimizing its effects on the hologram [Ref. 5].

B. COMBUSTION BOMB AND MASTERSIZER

The high quality optical windows and relatively small diameter of the combustion bomb used for holography made it possible to also use the Mastersizer for direct measurement of particle sizes and distributions immediately after ignition of the propellant strand. The combustion bomb was mounted horizontally into the optical path of the

Mastersizer. The diameter of the bomb dictated the use of a 300 mm Fourier transfer lens and, therefore, a minimum measurable particle size of 1.0 microns. The ignition process was identical to that previously described, although a slightly greater purge rate was used to limit obscuration of the lower powered Malvern laser. Based on burn rates described in the Burn Rate Determination Results section of this thesis, the number of sweeps possible during the burn of any of the propellants could be determined. The sweep time of the Malvern system, to include processing, was estimated at 7 milliseconds per sweep. Specifically, this procedure was attempted using the 4.68% and 16% Al loaded propellants at a pressure of 500 psi. Propellant strands of 6 x 5 x 2 mm dimensions were selected and 60 measurement sweeps were attempted. The measurement sweeps were initiated using the Malvern keyboard from behind the control booth, immediately after ignition of the propellant grain.

C. RESIDUE COLLECTION

Particle collection was conducted in the larger combustion bomb which allowed use of a collection cup. The combustion bomb and the collection cup were cleaned prior to each firing with acetone. The collection cup was placed in the combustion bomb and the ignition wire was positioned in contact with the propellant strand. A propellant strand generally 8 millimeters in width, 8 millimeters in height,

and 5 mm in thickness was used for all particle collections. A fluid was funneled into the bottom of the collection cup to a depth of 0.5 inches. Distilled water was used for the quenching medium for both propellants. One sample of 4.68% aluminum was also collected in an ammonium acetate buffered isopropyl alcohol quench to verify the negligible effect of using water as a medium for holding aluminum oxide [Ref. 7]. The combustion bomb was pressurized with nitrogen with the purge turned on slightly to insure that all oxygen was removed; then the purge was shut off during propellant strand burnings. Collections were made at 100 psi, 250 psi, 500 psi, and 750 psi for all but the 16% Al propellant, which was only collected at 250 psi and 500 psi.

After each firing was completed, the residue was washed with methanol into a glass beaker and allowed to settle for eight hours. Methanol was then siphoned off until only a small amount was left covering the residue. New methanol was added to the beaker and it was placed in an ultrasonic cleaner for 15 minutes. The sample was then allowed to stand for eight hours again, and the process was repeated until the methanol was completely clear after an eight hour settling time [Ref .

D. RESIDUE PARTICLE SIZING

Residue samples collected from the non-holographic combustion bomb were analyzed using the previously described

Malvern Mastersizer light scattering measurement system. To achieve resolution of 0.1 micron, the system employs a 45 mm focusing lens, a 2.2 mm thick sample cell and reverse Fourier optics. The Malvern Corporation markets a small sample presentation unit which stirs and pumps the sample through the sample cell. This unit was not, however, available during the duration of these experiments. After lengthy efforts to validate the ability of the system without such a presentation unit (See Appendix A), analysis of all collected samples was conducted. Additionally, samples were collected and analyzed to investigate concerns in two areas of the collection process. First, a sample of ZrC loaded propellant at 250 psi was collected without any quench medium. This was done primarily in an effort to determine the significance of particles impacting on the collection vessel walls rather than into the quench medium. Secondly, concern has been expressed over the use of water as a quenching medium for aluminum combustion products [Ref. 6]. It is believed possible that the resulting HCl acid corrodes available free aluminum. Therefore, a sample of 4.68% Al loaded propellant at 250 psi was collected in a buffering quench medium consisting proportionally of ammonium acetate (40 grams) in (50 ml of) water and (approximately 950 ml of) isopropyl alcohol [Ref. 6]. Samples were

introduced into the sample cell as outlined in Appendix A. Obscuration levels of approximately 30% to 50% were achieved whenever the quantity of collected particles was sufficient.

E. SEM SAMPLE PREPARATION AND MICROSCOPY

Initially, an eyedropper was used to extract a representative sample of each propellant at each pressure while it was magnetically stirred awaiting light scattering measurements. This, however, provided low particle concentration, requiring many photographs to acquire an appreciable total particle count. Subsequently, an ultrasonic stirrer was employed to suspend collected samples in a lesser amount of water; thereby providing the means of extracting a highly concentrated representative sample for SEM examination. These small samples were then dripped onto highly polished pedestals where they were allowed to naturally dry, or were oven dried. The residue samples were then gold plated for 30 seconds in a DSM-5 sputter module to obtain a thin, even coating of gold. This was necessary to achieve the good conduction required for SEM examination, which was done using an accelerator voltage of 20 kV and type 52 Polaroid film. A 90 degree incidence beam was used for all photographs, and a scale factor was automatically labeled in microns by the SEM.

F. BURN RATE DETERMINATION

Knowledge of the burning rate of each propellant was useful for understanding the combustion process and assisting the experimental procedures where timing was important. The larger of the two combustion bombs was connected through a pressure transducer to a Hewlett-Packard Moseley 7100B Autograph model strip chart recorder. By measuring the time elapsed from initiation of the pressure rise due to ignition, to the point in time where the rise ceased, it was possible to use the grain length to determine the specific burn rate for each propellant at specific pressures. By observing the burn rate at various pressures, it was possible to approximate the coefficient (a) and exponent (n) in the expression

$$r=ap^n \quad (1)$$

where r is the burn rate in ins/sec and p is the pressure in psia.

IV. RESULTS AND DISCUSSION

A. COMBUSTION BOMB AND HOLOGRAPHY

The design of the combustion bomb used in the holographic investigation was driven by the desire to minimize speckle size and, therefore, improve the resolution of the hologram. This was to be achieved using as large a diameter illuminating beam as possible through a relatively narrow field of view. The resolution of this system was approximately 14 microns in the dynamic viewing of burning particles. Several low magnification photos of reconstructed holograms (to show the entire strand) are shown in Fig. 13. Because of this resolution limitation, the holographic technique failed to provide sizing data for the great majority of particles. Thus, it provided only a limited basis for comparison with the other methods of particle sizing which were utilized. This system did, however, provide a unique, permanent, visual record of the larger particles leaving the burning propellant surface. Specifically, examination of the 4.68% Al propellant revealed at least eight particles, ranging in diameter from 28 to 168 microns. Similarly, examination of the 16.0% Al propellant clearly displayed at least 25 particles in the 28 to 168 micron range. Of these, eight were approximately 56 microns and four more were approximately 84 microns in diameter. The

presence of these particles during one short (50 nanosecond pulse period) observation time of the entire burn suggests that sufficient numbers of such large particles exist and should be observed by the other techniques for particle sizing.

B. COMBUSTION BOMB AND MASTERSIZER

The concept of making light scattering measurements through the plume of a burning propellant strand offers several seemingly unsurmountable challenges. The desire for submicron resolution demands the use of short focal length collecting lenses. Naturally, the particles to be observed must then be within the short focal length of the lens. Realistically, however, combustion bombs require sufficient cylinder thickness to support the desired operating pressures. Specifically, the combustion bomb designed for the holographic investigations had an inner diameter of only 2.75 inches, but an outer diameter of 4.25 inches. These dimensions required the use of a 300 millimeter Fourier transfer lens in the Mastersizer. This lens provided resolution down to 1.2 microns. The relative narrowness of this bomb, however, created the requirement for a purge rate sufficiently high so as to prevent particles from impinging on the inner window surfaces. If the primarily submicron particles on the outside of the particle cloud succeeded in reaching the windows, artificially high obscuration and significantly biased particle data would result.

The need for any purge flow, let alone a relatively high purge rate, however, prevented this system from providing any usable data. The temperature gradients created by the purge flow and hot particles/gases leaving the burning strand resulted in severe beam steering of the illumination laser beam. This beam steering was evident in the light energy displays of each measurement effort. The actual effect of the beam steering is to mask the presence of the larger particles. The light scattered by these larger particle occurs primarily at small forward angles, at the same location where the intensity from the beam steering is seen. Exclusion of the 10 affected inner diode rings was possible through a "kill data" feature in the Mastersizer software. Of three tests conducted with 16% aluminum propellant at 500 psi, one experienced splattering of particles on the windows, and all three demonstrated significant beam steering. Without the "kill data" option applied, D_{32} values of 15 and 303 microns were observed. With the "kill data" applied to the first 10 diodes, these values were reduced to 4 and 164 microns. In either case, results were inconsistent and not usable.

Overall, the inability of this system, as configured, to measure either submicron or moderately large particles prevented it from providing any useful particle information. One possible solution to this problem would be to use a smaller illumination beam diameter and/or a wider propellant

strand in order to eliminate the large density gradients that exist at the edge of the strand. A second possible solution would include heating of the purge flow to reduce the gradient, however, this would likely influence the burn rate of the propellant.

C. RESIDUE COLLECTION

The method of residue collection described in the previous Experimental Apparatus and Experimental Procedures sections can also introduce uncertainty in the particle size data. Of primary concern was the affect of quenching on the particles leaving the burning strand. The distance to the quenching medium was kept as constant as possible. However, different burning rates at the various pressures could have resulted in some inconsistency in this distance. The effect of particles which had impacted upon the collection wall surface without any quenching can further affect the accuracy of the particle size data. This appeared to occur most for the propellants with higher aluminum concentrations and at higher pressures, suggesting that the burning rate of the strand influenced the fraction of particles emitted down into the quench versus out to the sides. For this reason one sample was collected without any quench. SEM and Mastersizer examination showed a D_{32} approximately twice that of the same propellant using a water quench. This is best explained by the escape of the submicron particles into

the purge flow. As previously mentioned, additional concern has been expressed over the chemical effects of quenching and of holding aluminum oxide particles in water for extended periods of time. This, however, was not believed to affect measurement efforts which do not depend on the weighing of free aluminum. SEM and Mastersizer measurements of a sample collected in a buffered ammonium acetate solution demonstrated negligible differences from those of the same sample quenched and collected in water.

Overall, the above mentioned factors were minimized throughout the collection process. While different metal loadings provided naturally different concentrations of particles, it was felt that thorough analysis of the residue could provide a basis for comparison and understanding of the trends in particle size behavior with pressure and propellant composition.

D. SEM RESIDUE RESULTS.

The use of a SEM provides an excellent means for analyzing small particle collections, either visually, or by automated data processing. It can also provide evidence of very large particles, which may not be detected using light scattering techniques. The limitation of this method is believed to be the capturing of a representative sample of particles for such detailed analysis. Efforts at minimizing

this source of inaccuracy included the selection of samples during stirring and the analysis of a sufficient number of particles.

Summaries of both D_{32} and D_{43} data from visual investigation of SEM residue photographs are included in Tables 2 and 3. (Particle counts between 498 and 1,256 were utilized) Figure 14 includes representative SEM photographs. Of noteworthiness in these photos is the consistently spherical particle shape of the aluminum loaded propellant residue (and the ability to easily identify particle size modes, i.e., significant presence of similar diameter particles), and the mixture of spherical and non-spherical residue from the ZrC propellant. Distribution plots obtained from the SEM photograph are superimposed on Mastersizer measurements of the same particles in Figure 15.

E. MASTERSIZER RESIDUE PARTICLE SIZING RESULTS

As noted in the Experimental Apparatus section, a circulating pump was not available to provide circulation of the sample. While the resolution of this system was 0.1 microns, the quality of data obtained was still dependent on representative samples being viewed. As is the case with any light scattering measuring device, large particles settling or not circulating with the much smaller particles will bias the data toward lower values of D_{32} . As previously noted, Figure 15 provides distribution plots of both SEM

and Mastersizer data. Sample Mastersizer outputs are included in Figure 16 and D_{32} and D_{43} data are integrated into Tables II and III respectively.

The values of D_{32} and D_{43} determined using SEM analysis were consistently less than the values obtained using the Mastersizer. It takes only a very few large particles out of a 1000 particle count from a SEM picture to greatly change D_{32} or D_{43} . SEM analysis of particle distributions are therefore of limited utility unless all particles are collected and screened.

Another interesting result from the Malvern data was that a dominant amount of particle mass (volume) appeared to be concentrated at a diameter of approximately 20 microns for all three of the aluminized propellants. In contrast, the ZrC exhibited a much broader peak near 20 microns, and had considerable mass concentrated above 30 microns. This latter distribution may be the result of the dominance of non-spherical particles.

F. BURN RATE DETERMINATION

Burn rate values for the two lower-level aluminum loaded propellants and the ZrC loaded propellant are summarized in Table IV. The 16% aluminum loaded propellant was designed to burn at .378 in/sec at 625 psi. The experimentally determined expression provided by the Thiokol Corporation was $r = (.040)p^{(.35)}$ [Ref. 7].

V. CONCLUSIONS AND RECOMMENDATIONS

A number of approaches were used to investigate the characteristics of the products of metallized propellant-strand combustion. Analysis of the results of each of these methods suggested serious shortcomings for each, and areas where each can be improved. When considered together, however, this variety of diagnostic techniques could provide a very complete picture of the behavior of combustion bomb products. While holography fails to provide insight into the overall particle size distribution, this method provides undisputable evidence of large particle presence during the strand burn. Improved resolution to the 5 micron range would greatly improve this technique. It would be equally desirable to be able to do real time light scattering measurements, using an instrument such as the Malvern Mastersizer. To make this useful, however, the challenges of beam steering must be overcome. Recommended changes include a smaller illuminating beam diameter, a larger propellant strand, heating of the purge flow, or possibly a laser source with different intensity and wavelength. Another possibility would be to develop an active control which could maintain the central position of the unscattered beam.

Collected residue was examined using both the Mastersizer's light scattering technique and SEM examination. The value of SEM exists solely in the ability to scan through a sample in search of large particles or consistent size modes, but not in any effort to obtain particle distributions. This is because pictures, regardless of how many, capture so small a fraction of the overall distribution that it would be very unlikely to be representative of the whole sample. Furthermore, several very large particles can have significant influence in the distribution characteristics of a given sample, but may either not be included in the SEM sample, or may not be able to be photographed due to overcharging in the SEM. Finally, Mastersizer analysis using light scattering techniques offers the best overall approach to capturing particle size distribution data. This method of examination, however, is only as good as the system which collects the sample and the system which presents it for illumination. In both cases, improvements are recommended. While the choice of medium used to collect the particles appeared insignificant, the challenge of completely and consistently capturing and quenching all particles appeared to be critical and unsatisfactory. Unfortunately, recommendations to overcome this problem, particularly with highly metallized propellants at high pressures, could only include a drastic change in the style of the combustion and collection vessel. A spinning collection system, similar to that

used at Morton Thiokol Corporation, would be an example. The problem of presenting the sample with both large and small particles properly suspended for illumination can be more easily overcome with the acquisition of a commercial pump and stir unit, or the assembly of one from commercially available parts. The overall results of these shortcomings was the failure of this system to identify any consistent trends, if they existed, as functions of either pressure or metal loading. In summary, if strand burning data is to be of any quantitative value for comparison with motor data, significant progress in methods of residue collection and particle analysis will be required.

APPENDIX A

MASTERSIZER VALIDATION

The Malvern Mastersizer is designed to provide particle sizing with resolution down to 0.1 micron when the 45 mm lens is used, and 0.5 micron utilizing the 100 mm lens. Choice of lens is a function of the range of particle sizes expected and of the sample cell thickness. Prior to analyzing collected residue samples, polystyrene spheres of known diameters were used to investigate several areas of concern. Initially, the accuracy of the system's ability to correctly identify the size of single size samples was examined. This examination was done with both lenses, using an obscuration within the desired range of 30% to 50%, and using the correct presentation for polystyrene spheres. Presentation codes are based on the index of refraction of the particle and the suspending medium, as well as the index of absorption of the particle. A limited selection of these codes are preprogrammed into the Mastersizer's computer and are advertised as most significant when submicron particle sizes are considered. Varying the presentation was also examined, therefore, to measure the range of influence due to this parameter. Additionally, the effects of varying

obscuration from levels of 10% to 95% was also investigated. Finally, a brief examination of multi-mode samples was conducted using both the 45 mm lens and the 100 mm lens.

The Mastersizer system's accuracy for measuring micron and sub-micron particles was, predictably, much better with the 45 mm lens than with the 100 mm lens. At the same time, it should be noted that when the 100 mm lens is used, particles in a sub-range below the 0.5 micron level of resolution are still detected, even though not very accurately observed and not output in the Mastersizer distribution plots. This is significant in understanding the system's interpretation of particle sizes and distributions when samples include particles outside the accurate range of a 100 mm or larger lens. Overall, the Mastersizer proved to be extremely accurate, given the uncertainties of known diameter particle size deviations and the non-availability of a Malvern designed stir and pump presentation unit. This latter condition required that one of the two sample cell ports be capped and that samples be introduced into distilled water in the 2.2 mm thick cell using an eye dropper. Rotating and shaking the cell distributed particles throughout the cell.

The effects of varying presentations were observed using a distribution of particles with a mean diameter of 1.0 micron. Several trends were evident in observing values of D_{32} and D_{43} with both the 45 mm and 100 mm lenses. Using the 100 mm lens, increasing values of index of refraction

resulted in decreasing values of D_{32} and D_{43} . These trends were similar using the 45 mm lens, however, high index of refraction values resulted in only slightly decreasing values of D_{32} and D_{43} . The values of D_{32} ranged from .65 to .79 with the 100 mm lens and .72 to 1.26 with the 45 mm lens. Also of noteworthiness were the distribution plots of the high index of refraction presentations using the 45 mm lens. These plots suggested a bimodal distribution of particles centered on the true 1.0 micron value.

Having examined the effect of varying presentation values, the actual presentation codes to be used for aluminum oxide (Al_2O_3) and zirconium oxide (Zr_2O_3) were determined. Based on indices of refraction of approximately 1.70 and 1.33 for Al_2O_3 and water respectively, and an index of absorption of Al_2O_3 approaching 0.0, the most suitable presentation code of 1400 was selected. An index of refraction of 2.05 and an index of absorption of .001 for Zr_2O_3 resulted in a presentation code of 1803. These codes were used throughout all Mastersizer analysis [Ref. 8].

The effects of varying obscuration were observed on samples of 1.0 micron particles and on a mixed sample of 1.0 and 0.5 micron particles. Throughout both, it was evident that increasing obscuration resulted in decreasing values of D_{32} and D_{43} . The range of observed D_{32} values for the 1.0 micron particles was .71 microns to .53 microns, and

similarly, 1.05 microns to .41 microns in the mixed sample. Finally, three mixed samples were measured and compared with data from each individual sample. While quantitative comparison could not be made without knowledge of particle concentrations, each distribution plot correctly reflected broadening due to the close, but different particle sizes.

Overall, the effort to validate the Mastersizer system demonstrated the system's reliability. And while gross errors in presentation or obscuration can most certainly prejudice measurements, variations within reasonable ranges resulted in only minor, if not negligible, differences. Additionally, this effort demonstrated the improved accuracy which use of the 45 mm lens provides when submicron size particles are present. Sample Mastersizer outputs are included in Figure 17.

TABLE I
PROPELLANT COMPOSITION

Constituents	2.00% Al	4.68% Al	16% Al	ZrC
Title	DD 1	DD 5	DD SS	ZrC
Gap (200-1)	14.67%	14.67%		
Tegdn (AK-17E)	8.49%	8.49%		
Aluminum (C003)	2.00%	4.68%	16.00%	
AP (200 micron)	47.45%	45.70%	69.85%	57.00%
AP (25 micron)	25.55%	24.61%		
AP (11 micron)				25.00%
R45M				8.851%
RDX				4.00%
Diocetyl Adipate				2.00%
Zirconium Carbide (5 micron nominal)				1.00%
DDI				1.76%
HB (binder)			14.00%	
Iron Oxide			0.15%	
Others	1.84%	1.84%		0.389%

TABLE II
D₃₂ DATA SUMMARY

	Mastersizer	SEM
DD1		
100 psi	4.20	3.51
250 psi	7.10	3.87
500 psi	6.84	4.86
750 psi	10.46	1.82
DD5		
100 psi	3.59	2.89
250 psi	7.98	2.41
500 psi	10.76	2.86
750 psi	4.91	3.48
250 psi (with Am Ac)	9.59	3.30
DDSS		
250 psi	19.25	7.01
500 psi	7.16	4.57
ZrC		
100 psi	9.74	6.66
250 psi	10.57	5.84
500 psi	7.48	4.17
750 psi	8.87	6.70
250 psi (w/o quench)	18.24	4.54

TABLE III
D₄₃ DATA SUMMARY

	Mastersizer	SEM
DD1		
100 psi	11.68	5.62
250 psi	25.94	5.88
500 psi	16.85	7.67
750 psi	22.02	2.44
DD5		
100 psi	13.91	4.20
250 psi	21.45	3.12
500 psi	22.07	5.11
750 psi	16.33	4.06
250 psi (with Am Ac)	20.42	4.22
DDSS		
250 psi	31.54	9.90
500 psi	18.86	7.65
ZrC		
100 psi	27.72	8.75
250 psi	22.70	7.01
500 psi	23.05	5.38
750 psi	15.57	8.17
250 psi (w/o quench)	34.17	5.72

TABLE IV
BURN RATE DATA (r; in/sec)

<u>Pressure (psi)</u>	<u>DD1</u>	<u>DD5</u>	<u>ZrC</u>
250	.437	.488	.222
500	.577	.673	.259
750	.647	.791	.340
value of n	.362	.442	.370



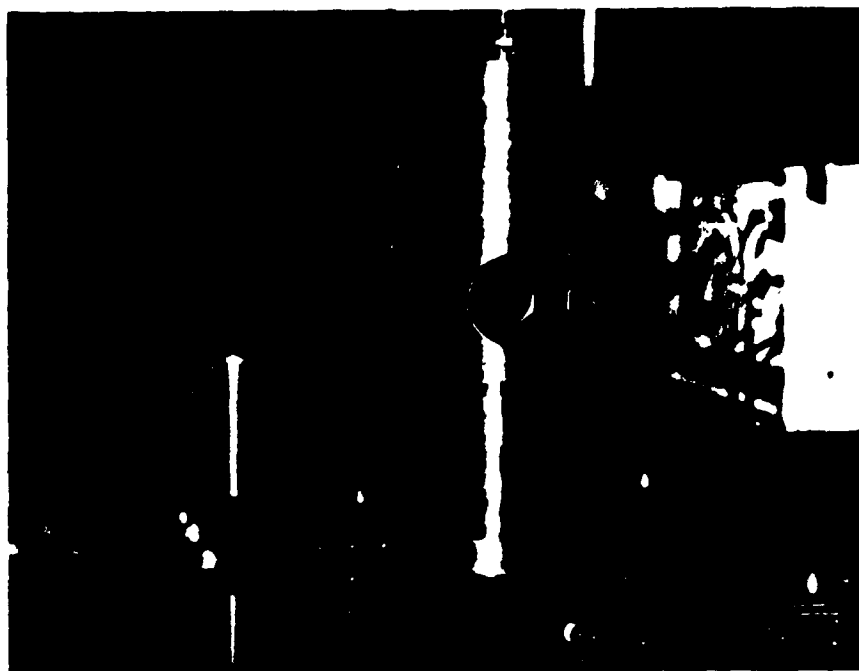


Figure 2. Holography Combustion Bomb

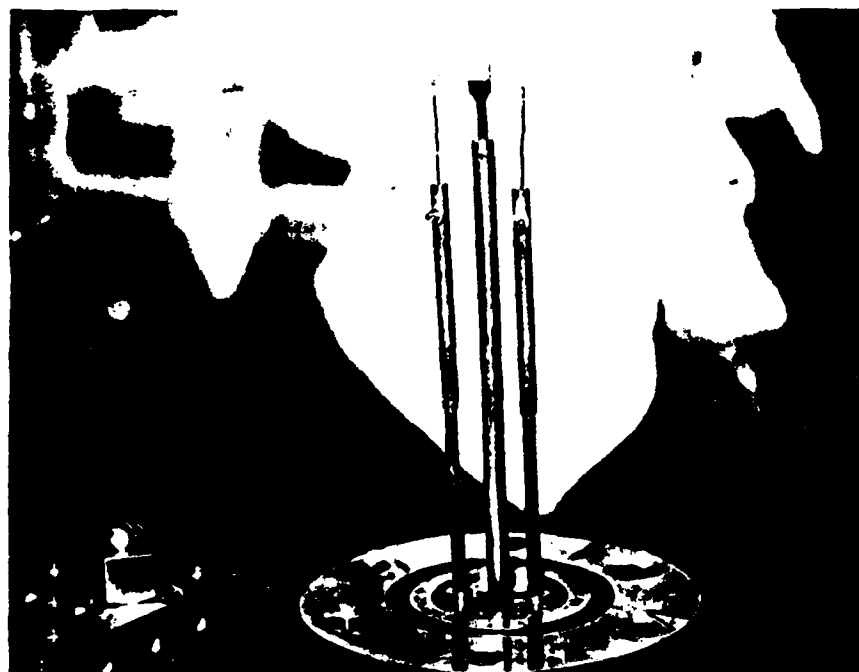


Figure 3. Holography Ignition Set-up

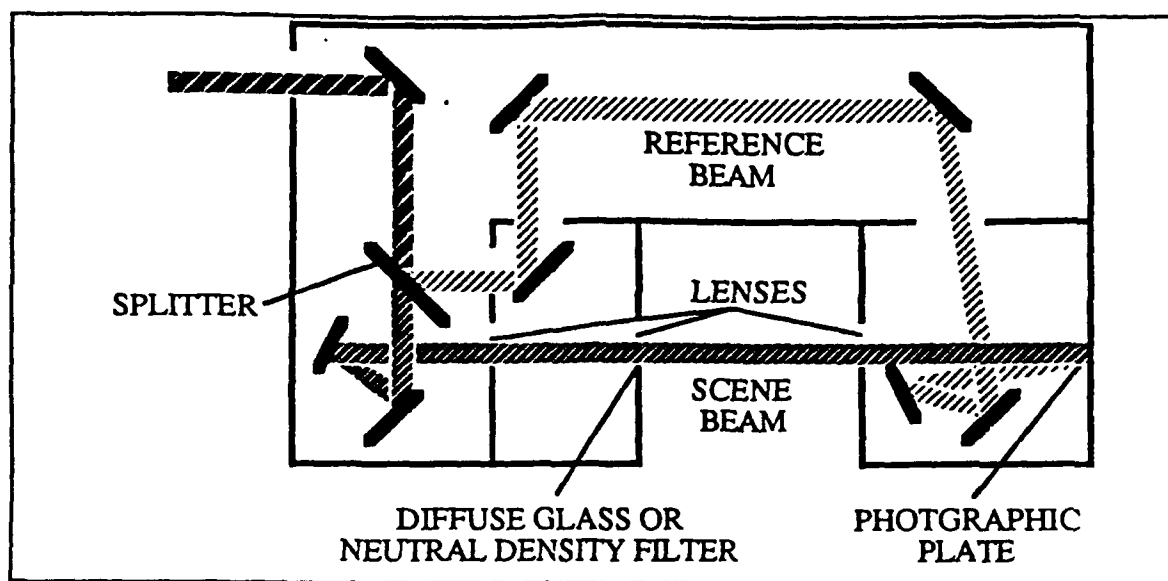


Figure 4. Holocamera Schematic [Ref. 9]

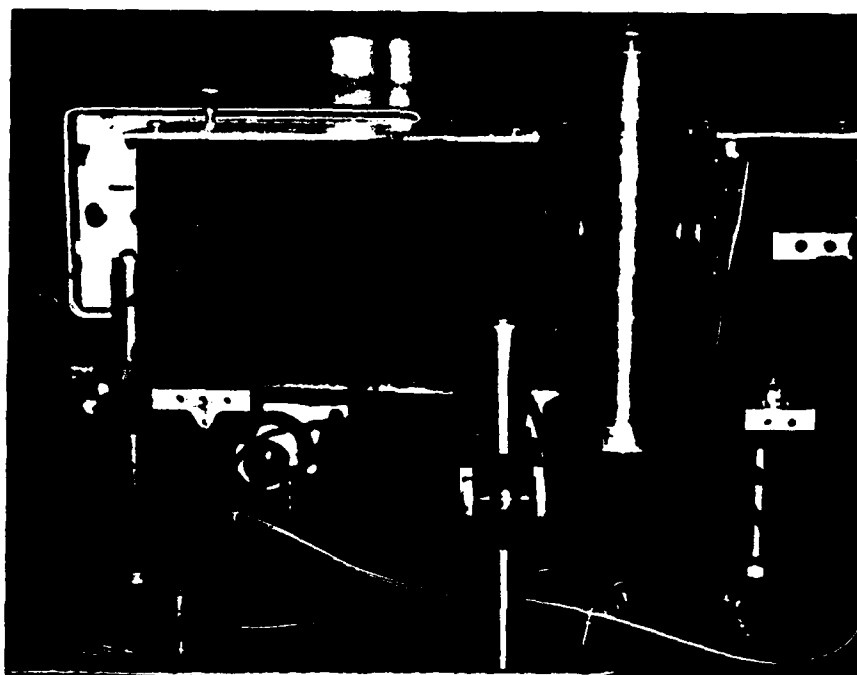


Figure 5. Laser, Holocamera and Combustion Bomb



Figure 6. Holography Reconstruction Setup



Figure 7. Combustion Bomb with Mastersizer

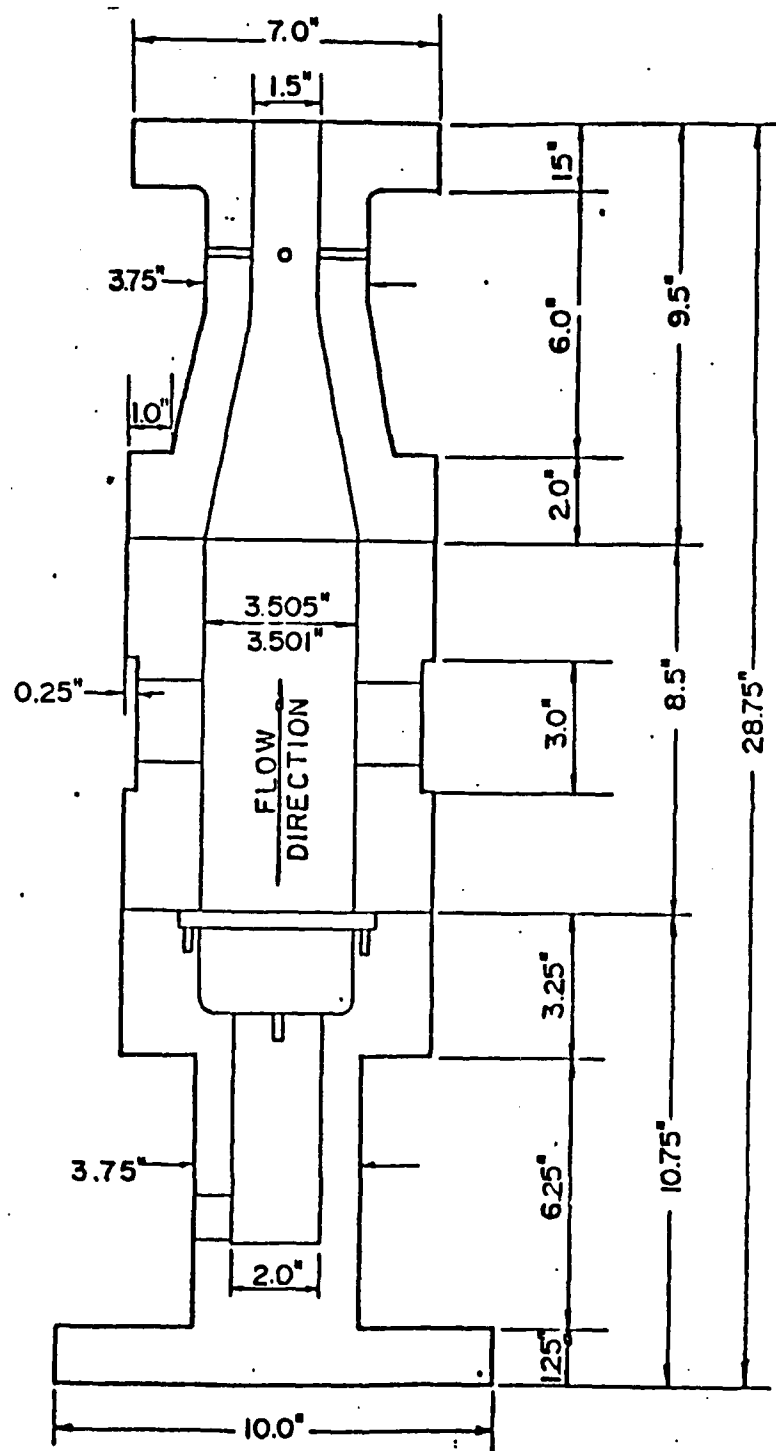


Figure 8. Collection Combustion Bomb Schematic

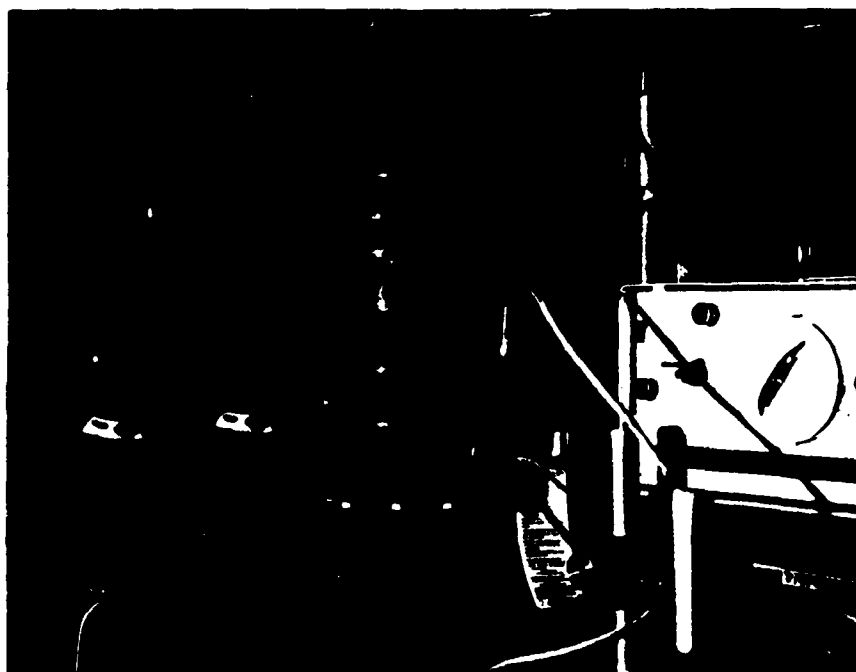


Figure 9. Collection Combustion Bomb

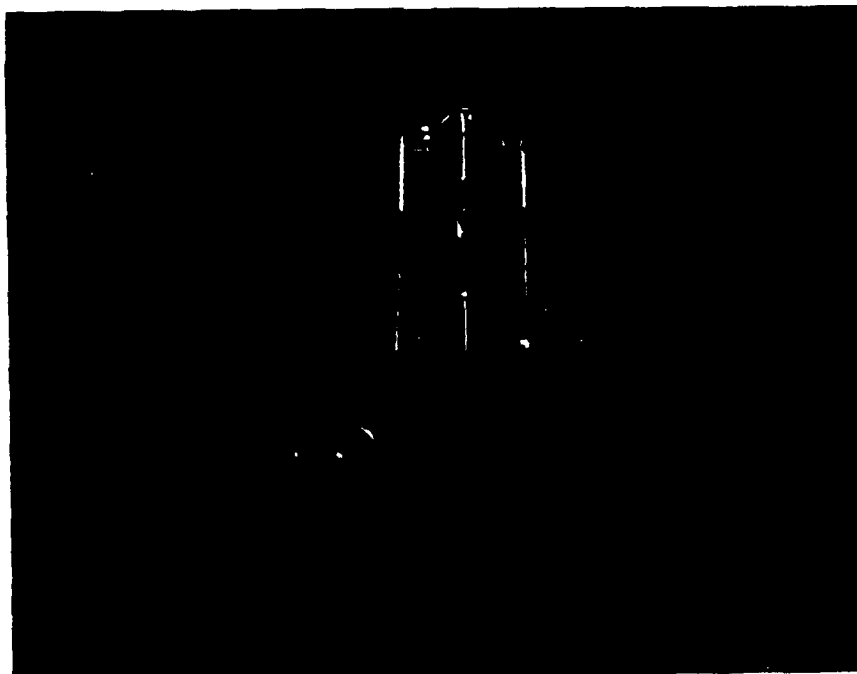


Figure 10. Collection Ignition Set-up

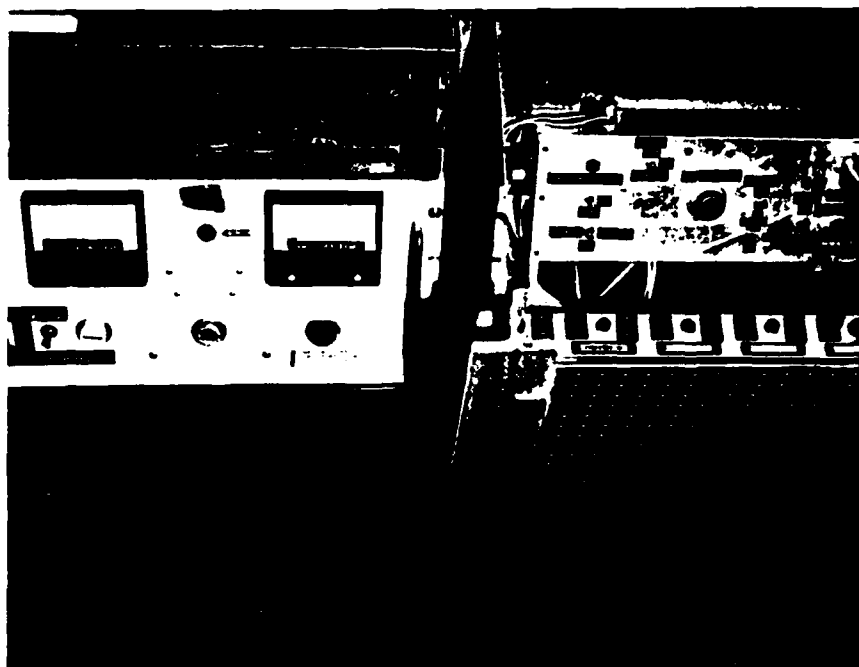


Figure 11. Remote Control Panels

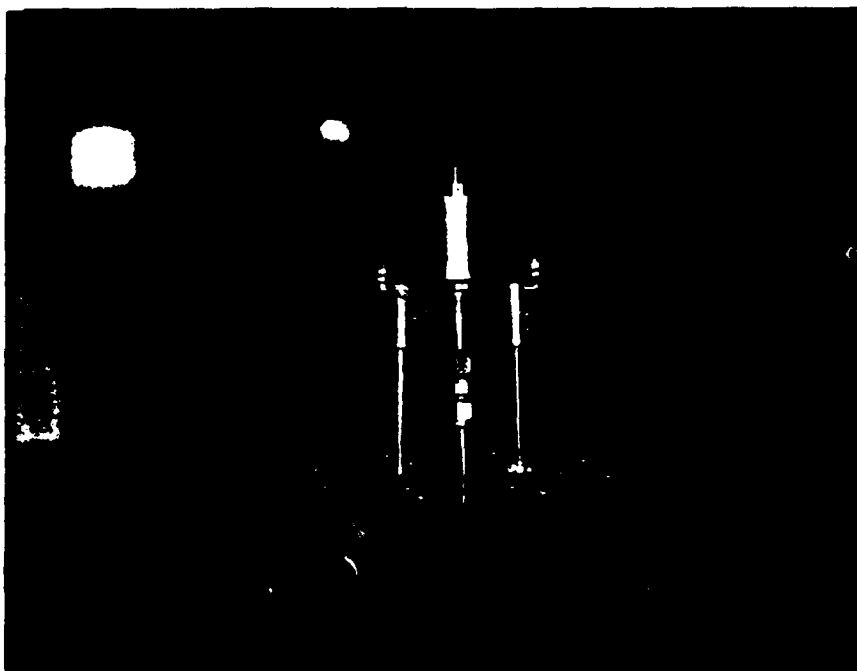


Figure 12. Residue Collection Setup

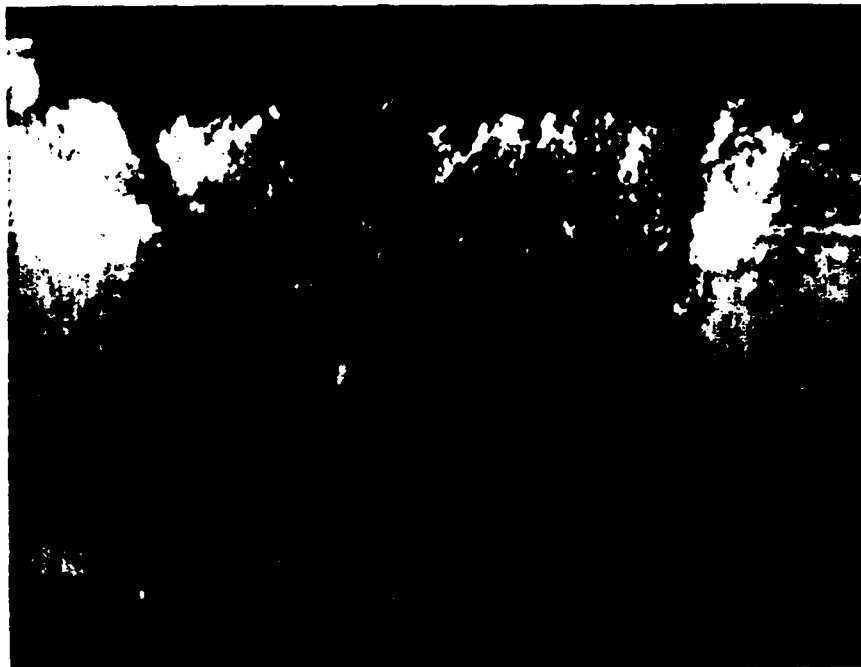


Figure 13a. Hologram of DD5 (x1 magnification)

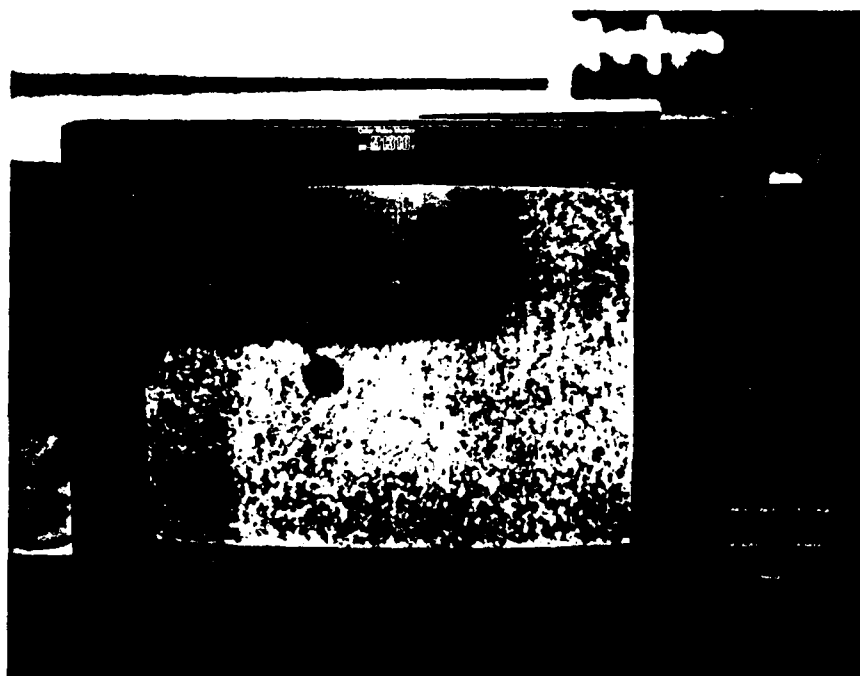


Figure 13b. Hologram of DD5 (x4 magnification)

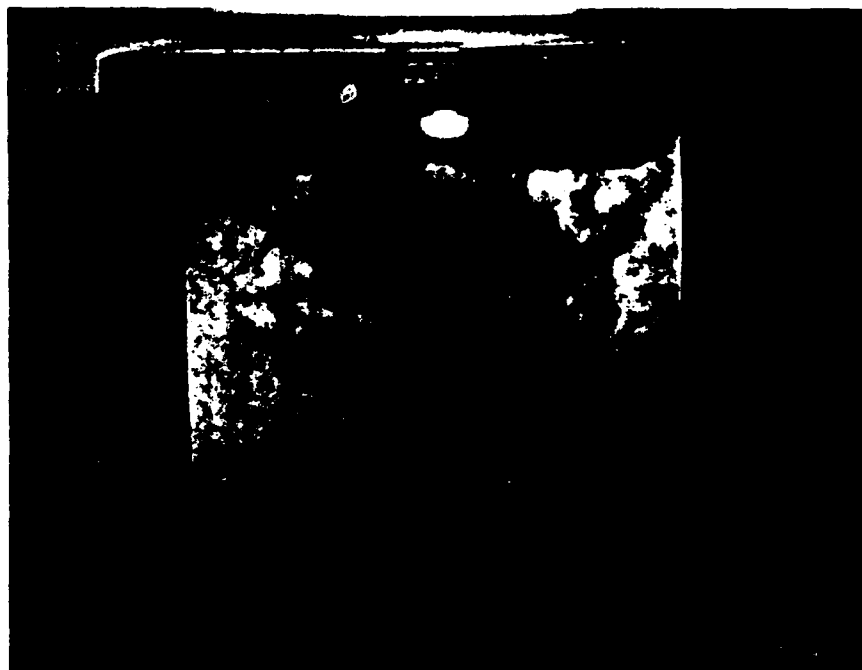


Figure 13c. Hologram of DDSS (x1 magnification)

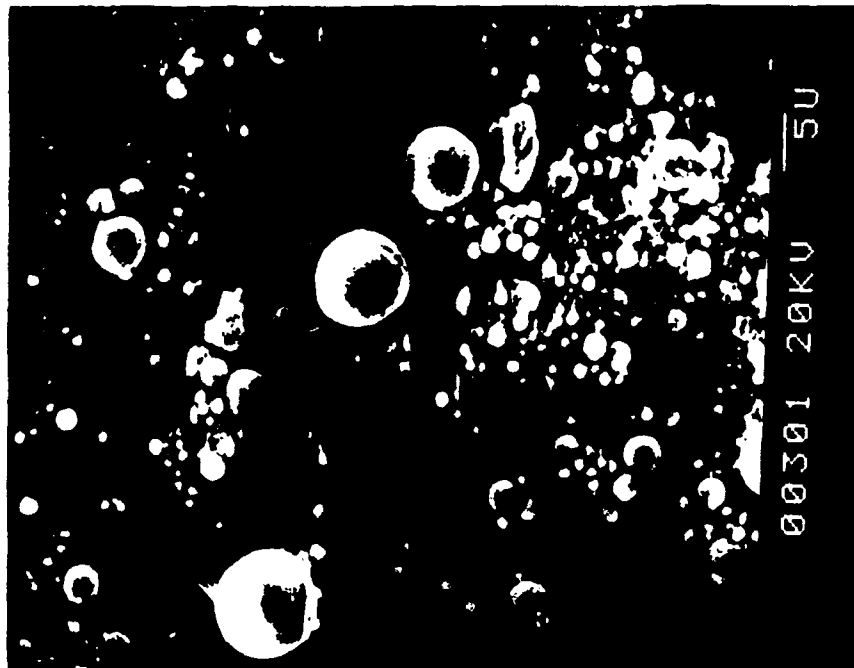


Figure 14a. SEM of DD1 at 100 psi

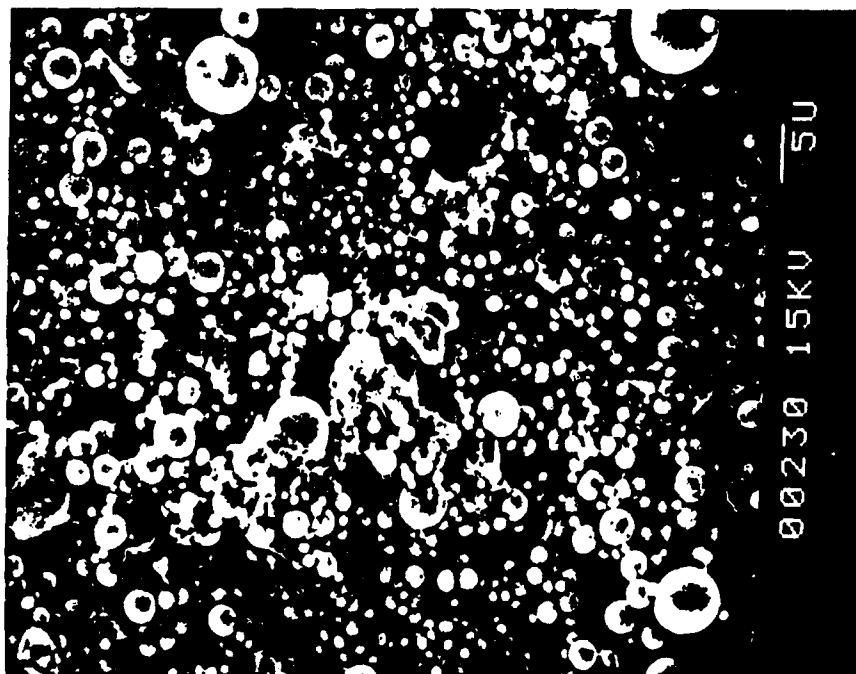


Figure 14b. SEM of DD1 at 250 psi

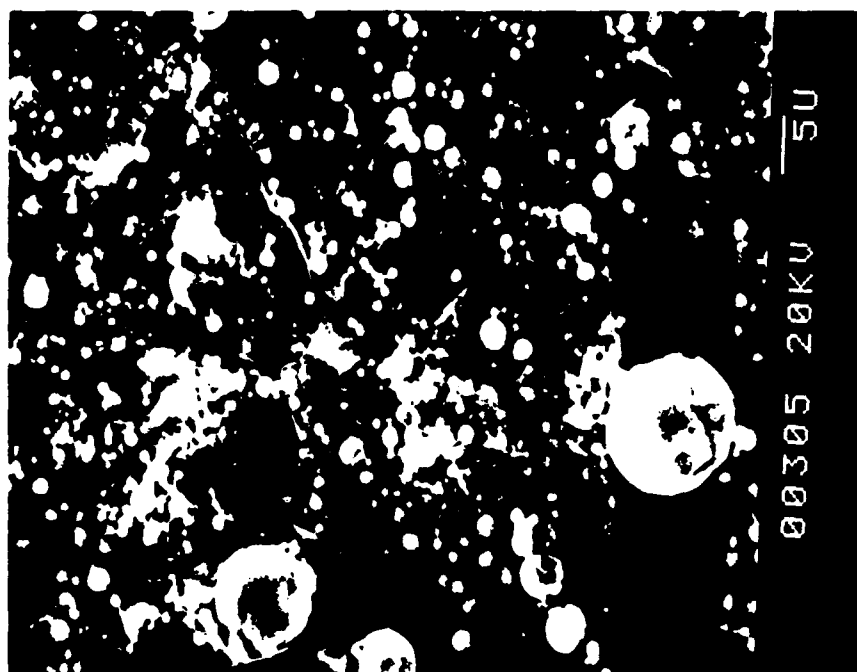


Figure 14c. SEM of DD1 at 500 psi

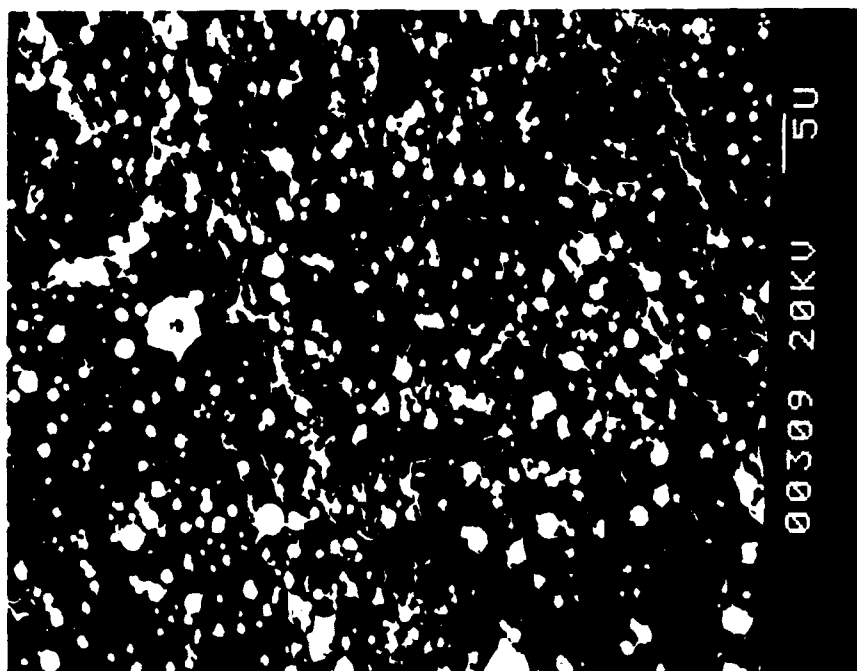


Figure 14d. SEM of DD1 at 750 psi.

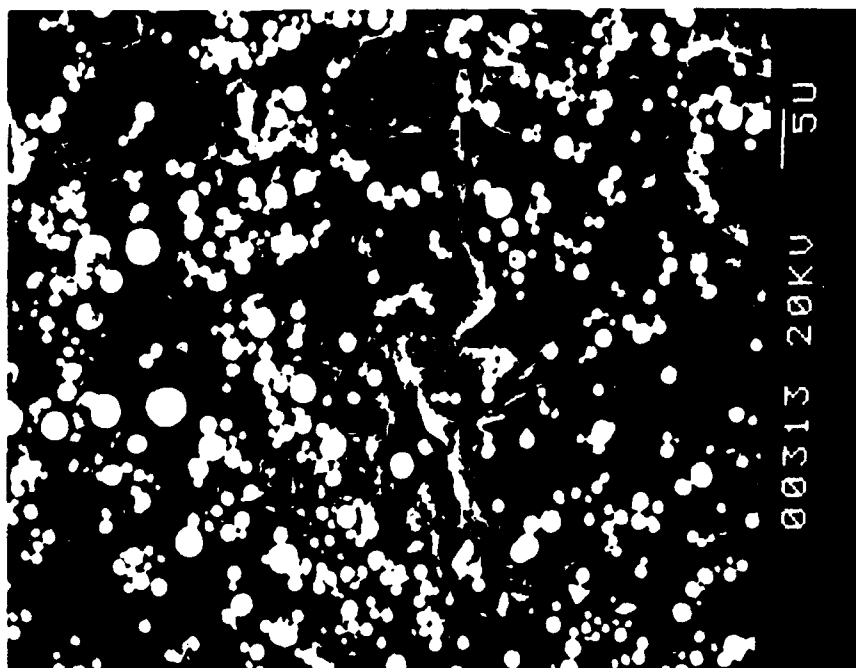


Figure 14e. SEM of DD5 at 100 psi

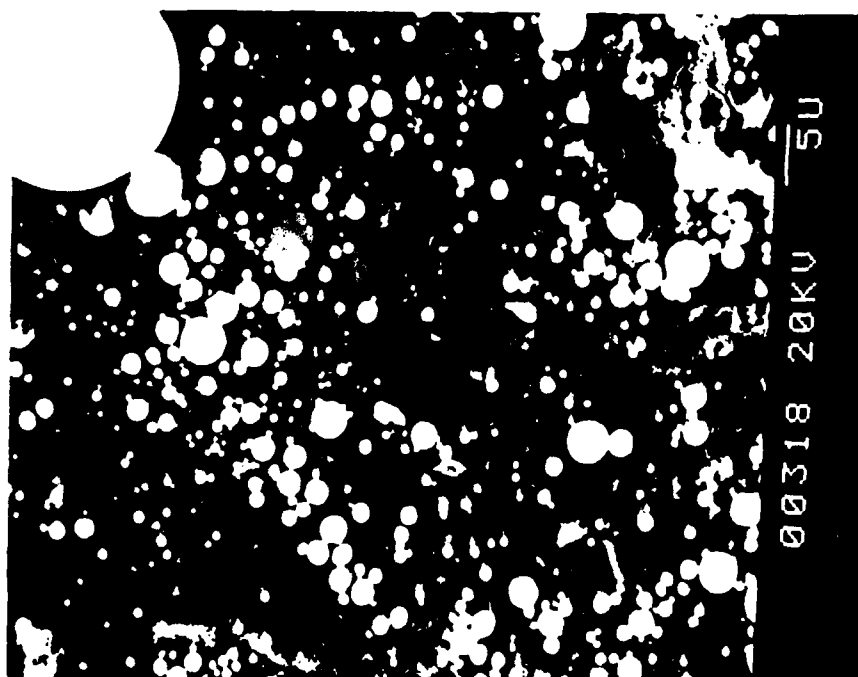


Figure 14f. SEM of DD5 at 250 psi

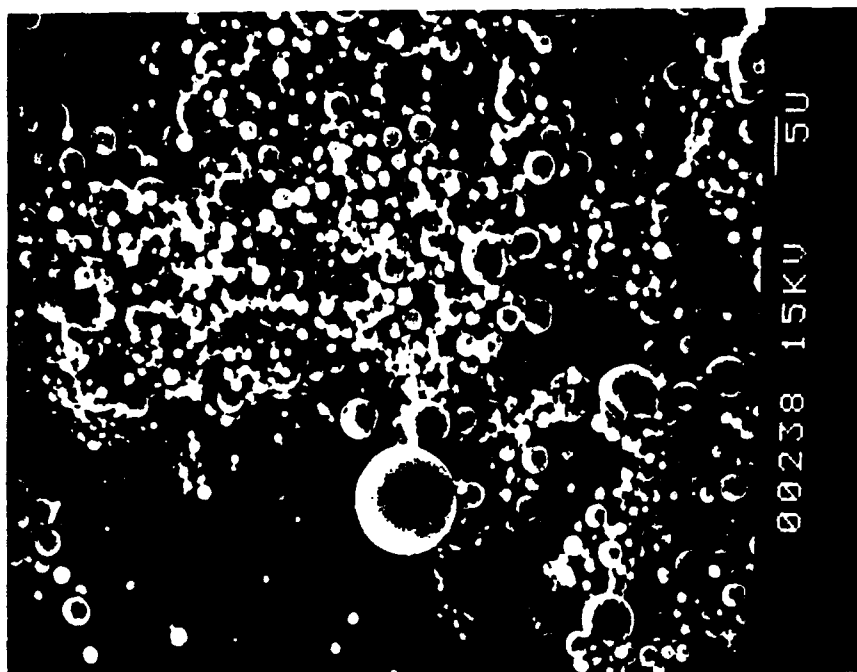


Figure 14g. SEM of DD5 at 500 psi

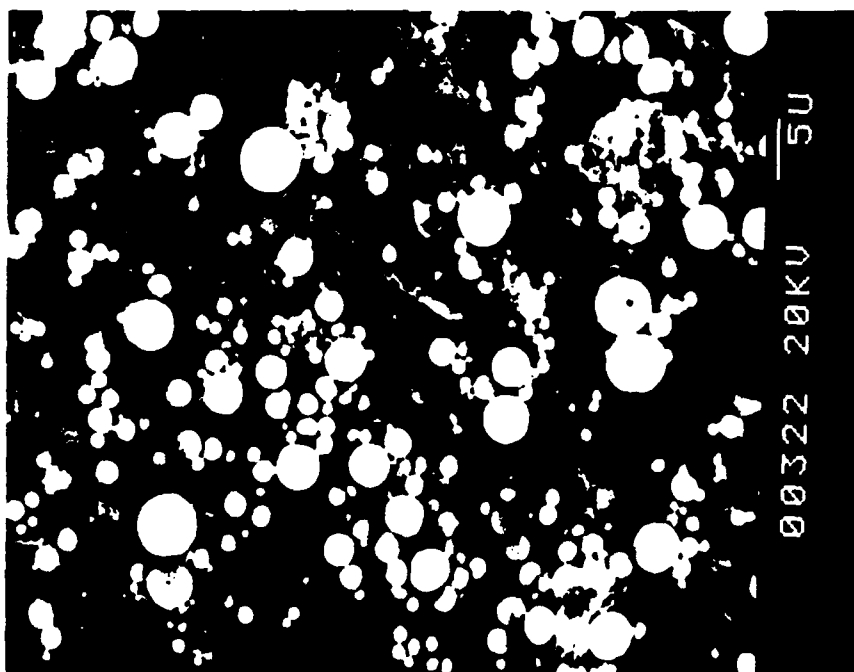


Figure 14h. SEM of DD5 at 750 psi

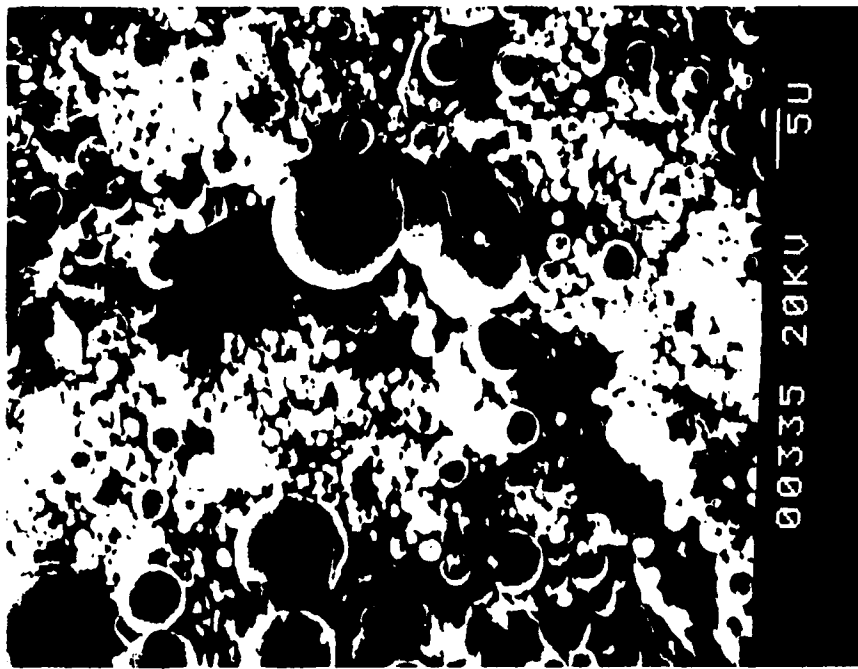


Figure 14i. SEM of DDSS at 250 psi

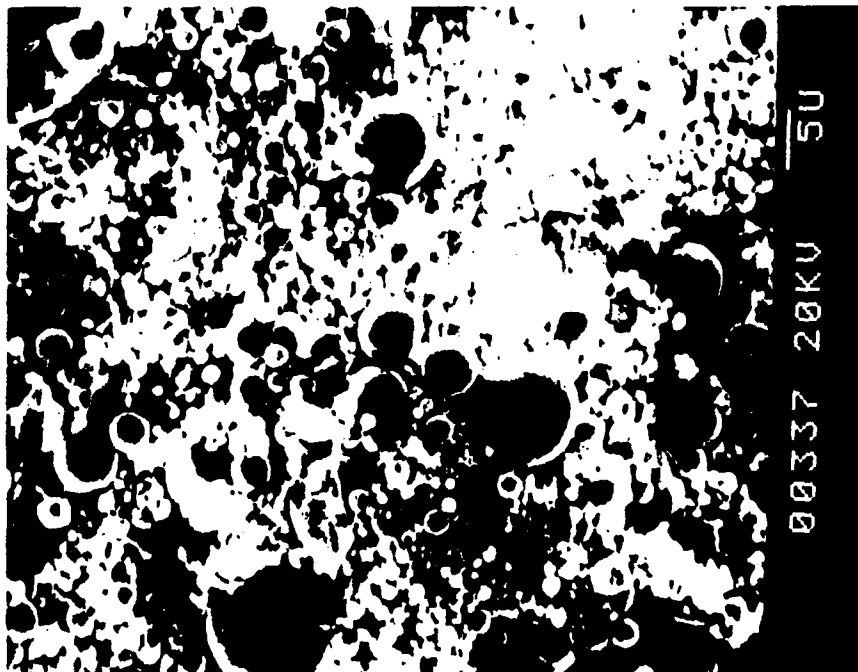


Figure 14j. SEM of DDSS at 500 psi

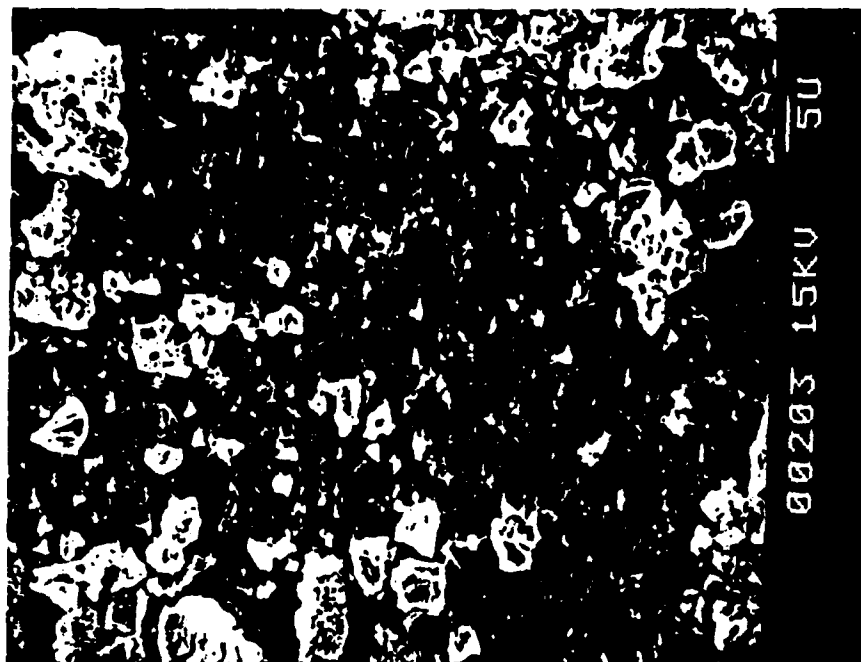


Figure 14k. SEM of ZrC at 100 psi

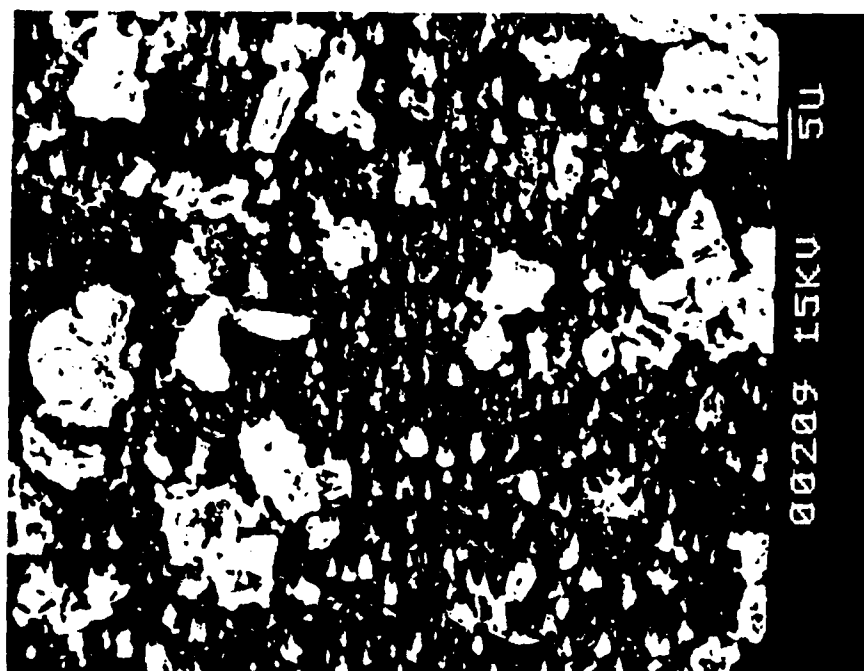


Figure 14l. SEM of ZrC at 250 psi

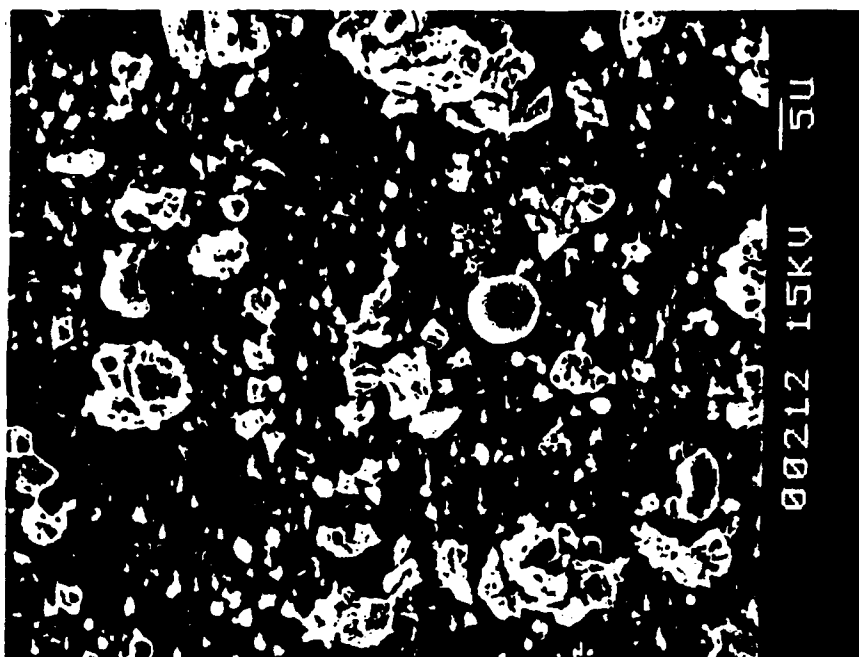


Figure 14m. SEM of ZrC at 500 psi

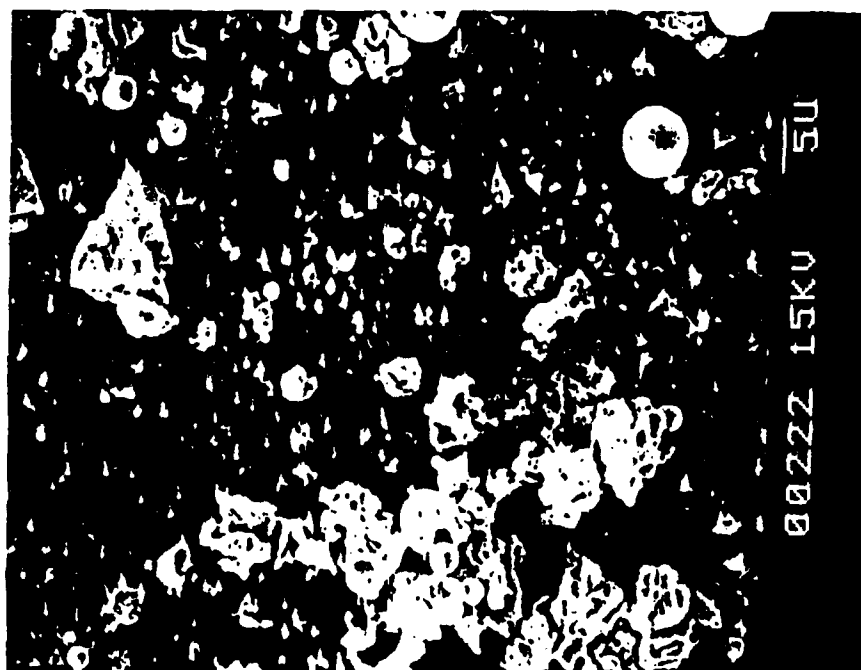
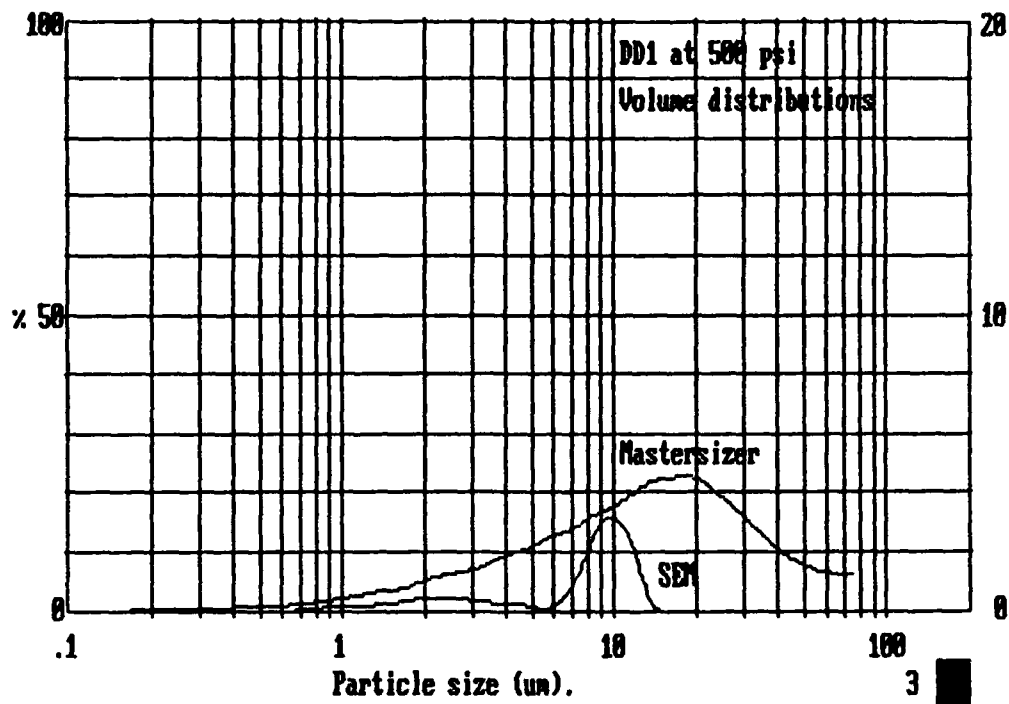
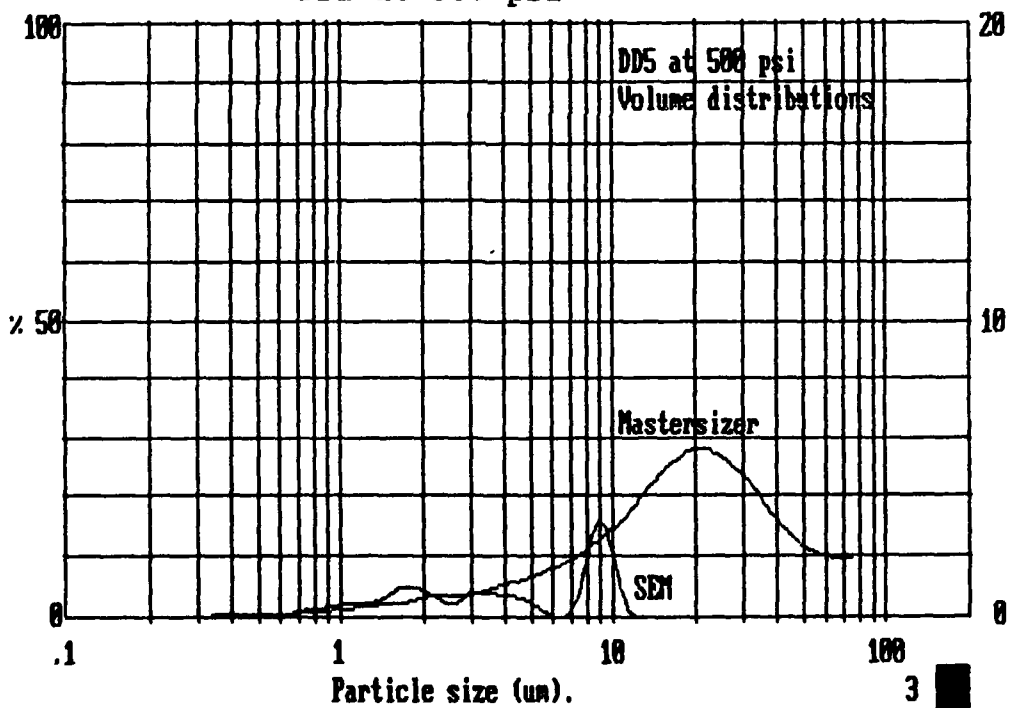


Figure 14n. SEM of ZrC at 750 psi



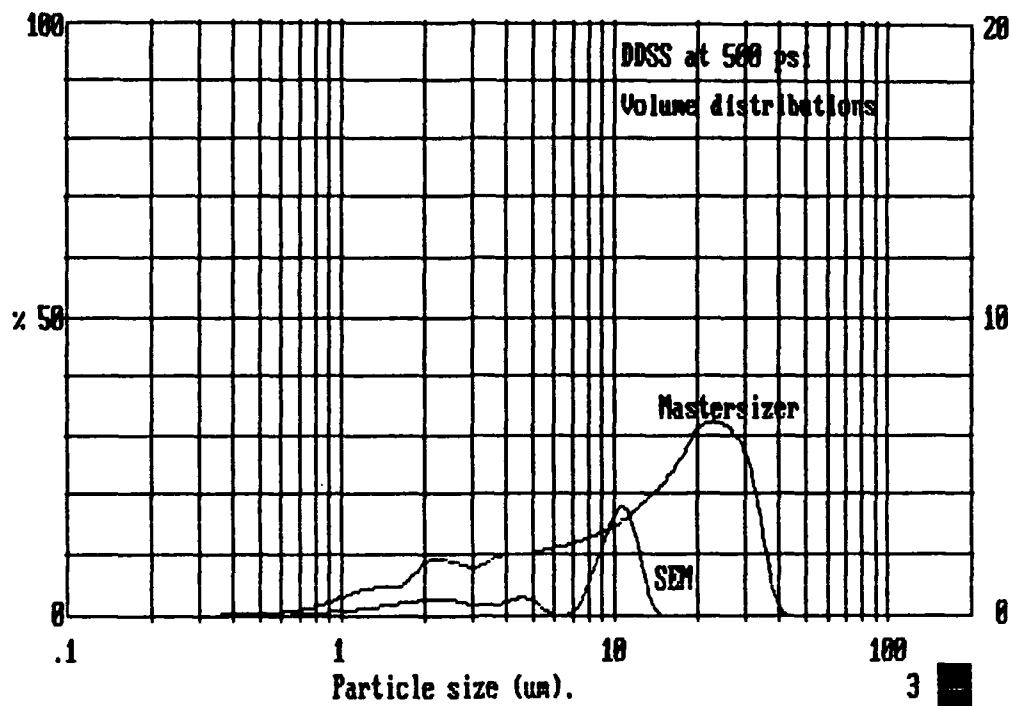
3769 1400 lgu376m

Figure 15a. Collection and SEM Numerical Comparison:
DD1 at 500 psi



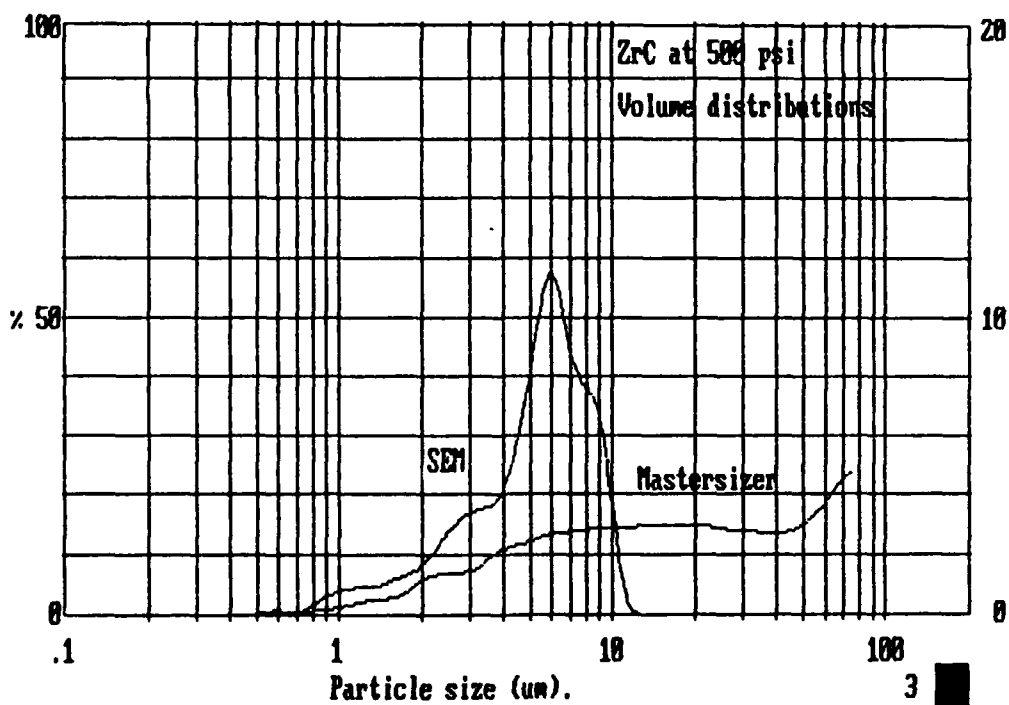
3769 1400 lgu376m

Figure 15b. Collection and SEM Numerical Comparison:
DD5 at 500 psi



3769 1400 lgu376m

Figure 15c. Collection and SEM Numerical Comparison:
DDSS at 500 psi



3769 1400 lgu376m

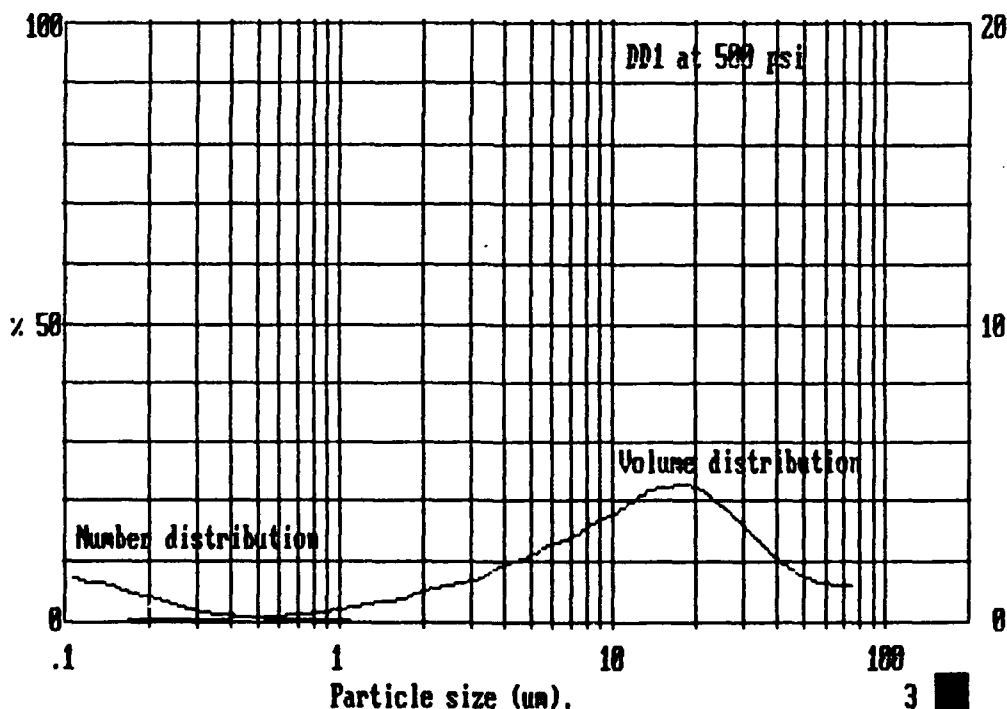
Figure 15d. Collection and SEM Numerical Comparison:
ZrC at 500 psi

MALVERN MasterSizer S3.01 Master Mode Fri 15 Dec 1989 10:57 am

Size µm. under	%	Size µm. under	%	Size µm. under	%	Size µm. under	%	Result source=bomb
0.10	0.0	0.55	1.3	2.98	12.1	16.3	59.0	Record No. = 3
0.11	0.0	0.61	1.5	3.32	13.5	18.1	63.6	Focal length = 45 mm.
0.12	0.1	0.68	1.7	3.69	15.2	20.1	68.2	Presentation =1400
0.14	0.1	0.75	2.0	4.10	17.0	22.4	72.6	Volume distribution
0.15	0.1	0.83	2.3	4.56	19.0	24.9	76.7	Beam length = 14.3 mm.
0.17	0.2	0.93	2.6	5.07	21.2	27.7	80.5	Obscuration =0.4315
0.19	0.2	1.03	3.1	5.64	23.6	30.8	83.8	Volume Conc. = 0.0065 %
0.21	0.3	1.15	3.6	6.27	26.1	34.2	86.8	Residual = 1.018%
0.23	0.3	1.28	4.2	6.97	28.9	38.1	89.3	Model indp
0.26	0.4	1.42	4.8	7.75	31.8	42.3	91.4	D(v,0.5) = 13.15 µm
0.29	0.5	1.58	5.5	8.62	35.0	47.1	93.2	D(v,0.9) = 39.33 µm
0.32	0.6	1.75	6.3	9.58	38.4	52.3	94.8	D(v,0.1) = 2.52 µm
0.36	0.7	1.95	7.2	10.7	42.0	58.2	96.2	D(4,3) = 16.85 µm
0.40	0.8	2.17	8.3	11.8	45.9	64.7	97.5	D(3,2) = 6.84 µm
0.44	1.0	2.41	9.5	13.2	50.1	71.9	98.8	Span = 2.8
0.49	1.1	2.68	10.7	14.6	54.5	80.0	100	Spec. surf. area 1.1905 sq.m./cc.

3769 1400 lgu376m

Figure 16a. Mastersizer Results of Collected DD1 at 500 psi



3769 1400 lgu376m

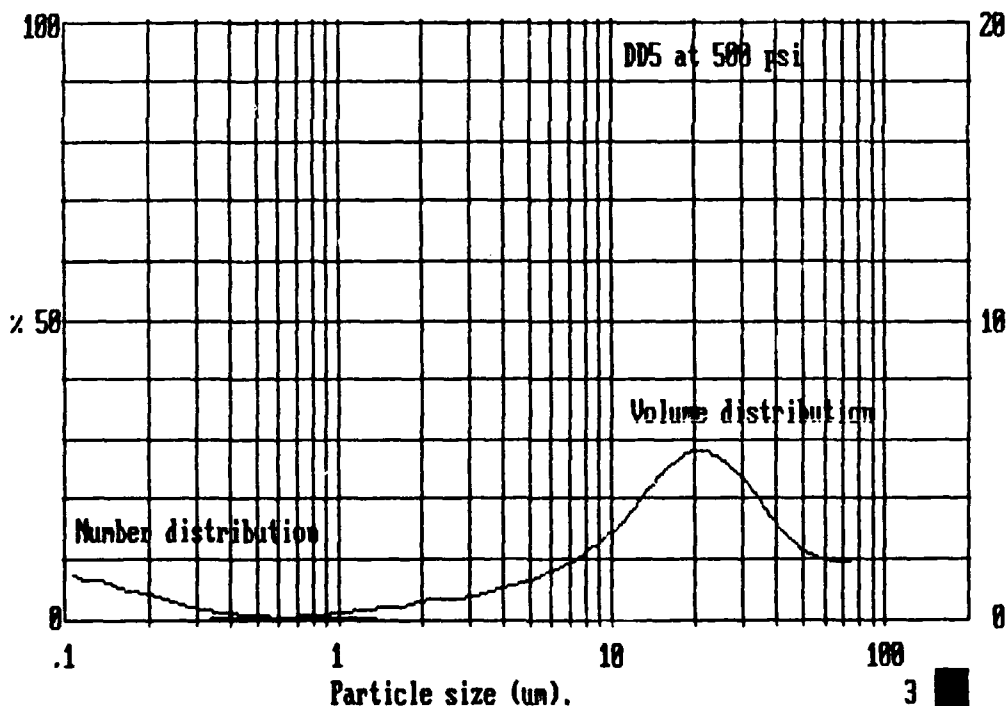
Figure 16b. Mastersizer Plots of Collected DD1 at 500 psi

MALVERN MasterSizer S3.01 Master Mode Fri 15 Dec 1989 11:04 am

Size µm. under	%	Size µm. under	%	Size µm. under	%	Size µm. under	%	Result source=bomb
0.10	0.0	0.55	0.5	2.98	6.8	16.3	43.3	Record No. = 7
0.11	0.0	0.61	0.6	3.32	7.5	18.1	48.5	Focal length = 45 mm.
0.12	0.0	0.68	0.7	3.69	8.5	20.1	54.1	Presentation =1400
0.14	0.0	0.75	0.9	4.10	9.5	22.4	59.8	Volume distribution
0.15	0.0	0.83	1.0	4.56	10.6	24.9	65.4	Beam length = 14.3 mm.
0.17	0.1	0.93	1.2	5.07	11.9	27.7	70.6	Obscuration =0.3068
0.19	0.1	1.03	1.5	5.64	13.3	30.8	75.5	Volume Conc. = 0.0064 %
0.21	0.1	1.15	1.8	6.27	14.9	34.2	79.8	Residual = 1.128%
0.23	0.1	1.28	2.1	6.97	16.7	38.1	83.6	Model indp
0.26	0.2	1.42	2.5	7.75	18.7	42.3	86.8	D(v,0.5) = 18.63 µm
0.29	0.2	1.58	2.9	8.62	21.0	47.1	89.6	D(v,0.9) = 47.94 µm
0.32	0.2	1.75	3.4	9.58	23.6	52.3	91.9	D(v,0.1) = 4.30 µm
0.36	0.3	1.95	3.9	10.7	26.6	58.2	94.1	D(4,3) = 22.07 µm
0.40	0.3	2.17	4.6	11.8	30.0	64.7	96.1	D(3,2) = 10.76 µm
0.44	0.4	2.41	5.3	13.2	33.9	71.9	98.1	Span = 2.3
0.49	0.5	2.68	6.0	14.6	38.4	80.0	100	Spec. surf. area 0.7510 sq. m./cc.

3769 1400 lgu376m

Figure 16c. Mastersizer Results of Collected DD5 at 500 psi



3769 1400 lgu376m

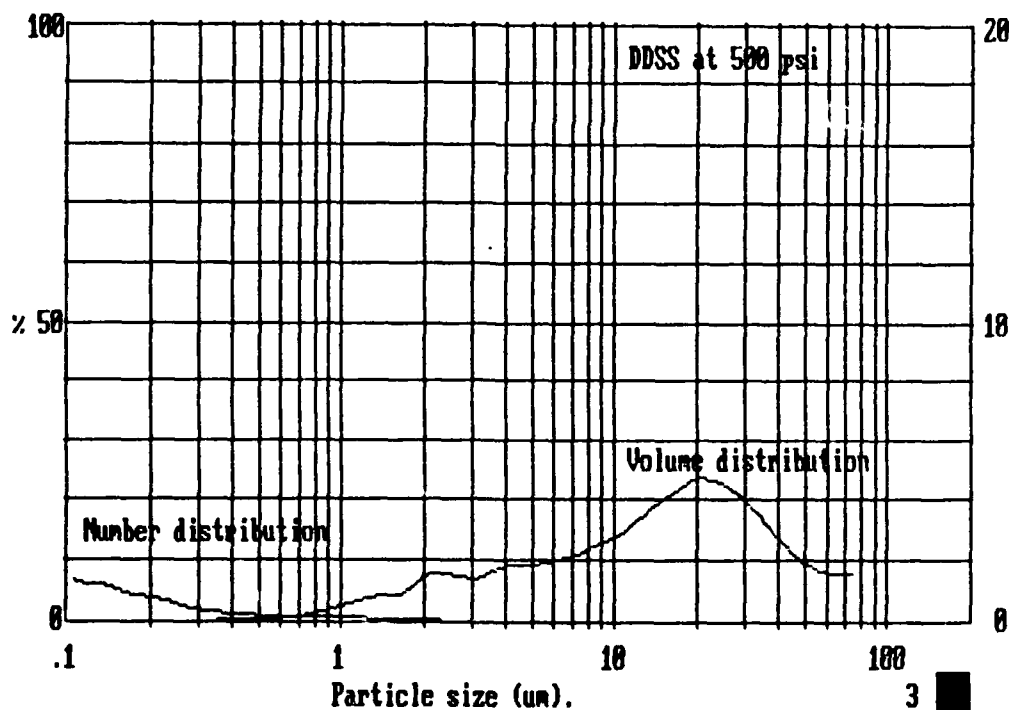
Figure 16d. Mastersizer Plots of Collected DD5 at 500 psi

MALVERN MasterSizer S3.01 Master Mode Fri 15 Dec 1989 11:11 am

Size µm.	% under	Size µm.	% under	Size µm.	% under	Size µm.	% under	Result source=bomb
0.10	0.0	0.55	0.5	2.98	13.5	16.3	52.4	Record No. = 16
0.11	0.0	0.61	0.6	3.32	14.9	18.1	56.8	Focal length = 45 mm.
0.12	0.0	0.68	0.8	3.69	16.5	20.1	61.4	Presentation = 1400
0.14	0.0	0.75	1.0	4.10	18.3	22.4	66.2	Volume distribution
0.15	0.0	0.83	1.2	4.56	20.1	24.9	70.8	Beam length = 14.3 mm.
0.17	0.0	0.93	1.6	5.07	22.0	27.7	75.3	Obscuration = 0.4099
0.19	0.1	1.03	2.1	5.64	23.9	30.8	79.4	Volume Conc. = 0.0063 %
0.21	0.1	1.15	2.7	6.27	25.9	34.2	83.2	Residual = 0.650%
0.23	0.1	1.28	3.5	6.97	28.0	38.1	86.4	Model indep
0.26	0.1	1.42	4.3	7.75	30.2	42.3	89.2	D(v,0.5) = 15.32 µm
0.29	0.2	1.58	5.2	8.62	32.6	47.1	91.5	D(v,0.9) = 43.83 µm
0.32	0.2	1.75	6.1	9.58	35.2	52.3	93.5	D(v,0.1) = 2.34 µm
0.36	0.2	1.95	7.3	10.7	38.0	58.2	95.2	D(4,3) = 18.86 µm
0.40	0.3	2.17	8.8	11.8	41.1	64.7	96.8	D(3,2) = 7.16 µm
0.44	0.4	2.41	10.5	13.2	44.5	71.9	98.4	Span = 2.7
0.49	0.4	2.68	12.0	14.6	48.3	80.0	100	Spec. surf. area 1.0191 sq.m./cc.

3769 1400 lgu376m

Figure 16e. Mastersizer Results of Collected DDSS at 500 psi



3769 1400 lgu376m

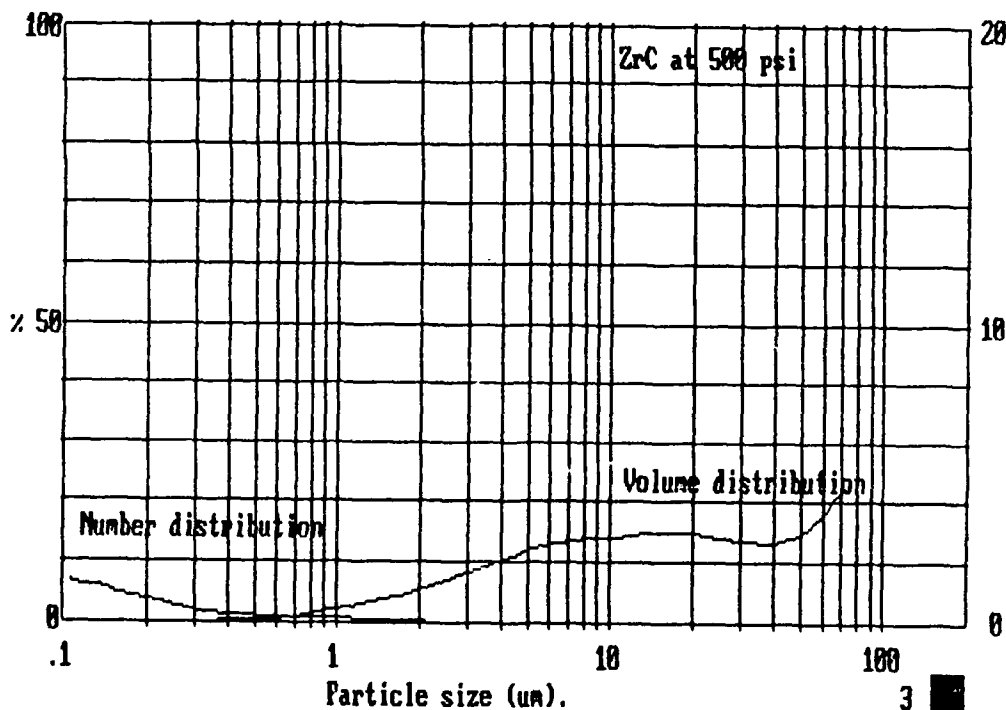
Figure 16f. Mastersizer Plots of Collected DDSS at 500 psi

MALVERN MasterSizer S3.01 Master Mode Fri 15 Dec 1989 11:08 am

Size µm.	% under	Size µm.	% under	Size µm.	% under	Size µm.	% under	Result source=boab
0.10	0.0	0.55	0.5	2.98	11.9	16.3	52.9	Record No. = 11
0.11	0.0	0.61	0.6	3.32	13.7	18.1	55.9	Focal length = 45 mm.
0.12	0.0	0.68	0.7	3.69	15.5	20.1	58.9	Presentation = 1803
0.14	0.0	0.75	0.9	4.10	17.5	22.4	61.9	Volume distribution
0.15	0.0	0.83	1.2	4.56	19.7	24.9	64.7	Beam length = 14.3 mm.
0.17	0.0	0.93	1.6	5.07	22.1	27.7	67.5	Obscuration = 0.1924
0.19	0.1	1.03	2.0	5.64	24.6	30.8	70.3	Volume Conc. = 0.0027 %
0.21	0.1	1.15	2.5	6.27	27.2	34.2	73.1	Residual = 0.925%
0.23	0.1	1.28	3.1	6.97	29.9	38.1	75.7	Model indp
0.26	0.1	1.42	3.8	7.75	32.6	42.3	78.4	D(v,0.5) = 14.68 µm
0.29	0.1	1.58	4.6	8.62	35.4	47.1	81.2	D(v,0.9) = 62.78 µm
0.32	0.2	1.75	5.5	9.58	38.3	52.3	84.2	D(v,0.1) = 2.61 µm
0.36	0.2	1.95	6.5	10.7	41.1	58.2	87.4	D(4,3) = 23.05 µm
0.40	0.3	2.17	7.6	11.8	44.0	64.7	91.1	D(3,2) = 7.48 µm
0.44	0.3	2.41	8.9	13.2	46.9	71.9	95.4	Span = 4.1
0.49	0.4	2.68	10.4	14.6	49.9	80.0	100	Spec. surf. area 0.9762 sq.m./cc.

3769 1803 lgu376m

Figure 16g. Mastersizer Results of Collected ZrC at 500 psi



3769 1803 lgu376m

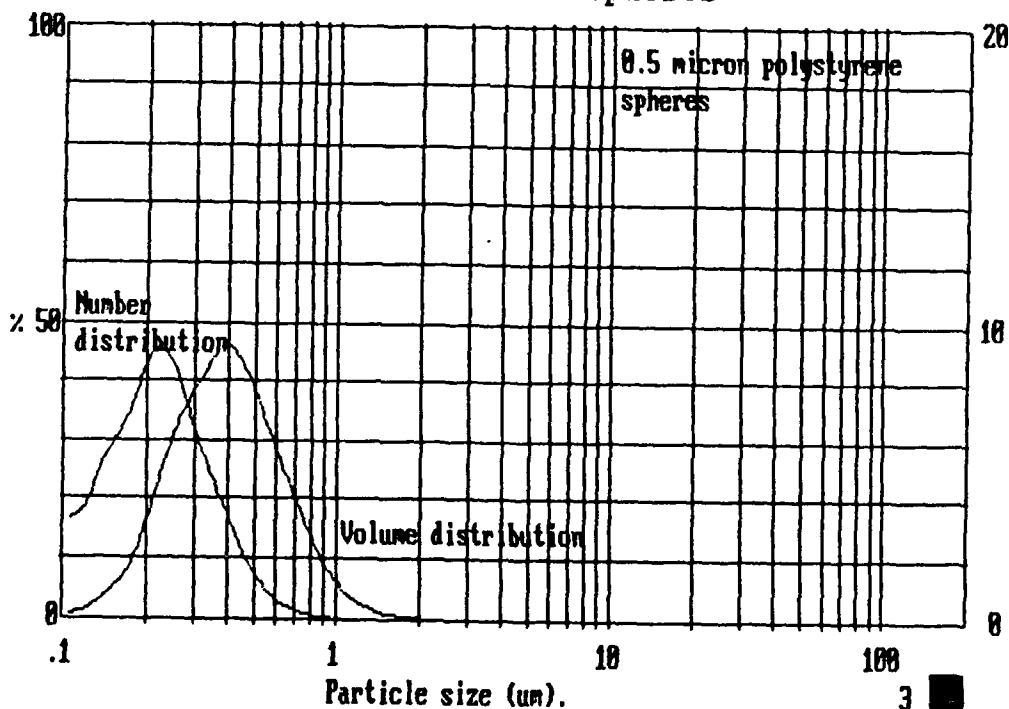
Figure 16h. Mastersizer Plots of Collected ZrC at 500 psi

MALVERN MasterSizer S3.01 Master Mode Sat 16 Dec 1989 12:43 pm

Size µm. under	%	Size µm. under	%	Size µm. under	%	Size µm. under	%	Result source=testy
0.10	0.1	0.55	76.5	2.98	100	16.3	100	Record No. = 23
0.11	0.3	0.61	82.6	3.32	100	18.1	100	Focal length = 45 mm.
0.12	0.6	0.68	87.6	3.69	100	20.1	100	Presentation =1000
0.14	1.1	0.75	91.5	4.10	100	22.4	100	Volume distribution
0.15	2.0	0.83	94.4	4.56	100	24.9	100	Beam length = 14.3 mm.
0.17	3.3	0.93	96.4	5.07	100	27.7	100	Obscuration =0.2861
0.19	5.3	1.03	97.7	5.64	100	30.8	100	Volume Conc. = 0.0012 %
0.21	8.5	1.15	98.6	6.27	100	34.2	100	Residual = 5.122%
0.23	13.1	1.28	99.2	6.97	100	38.1	100	Model indp
0.26	19.1	1.42	99.5	7.75	100	42.3	100	D(v,0.5) = 0.39 µm
0.29	26.1	1.58	99.7	8.62	100	47.1	100	D(v,0.9) = 0.72 µm
0.32	33.9	1.75	99.8	9.58	100	52.3	100	D(v,0.1) = 0.22 µm
0.36	42.4	1.95	99.9	10.7	100	58.2	100	D(4,3) = 0.43 µm
0.40	51.6	2.17	99.9	11.8	100	64.7	100	D(3,2) = 0.36 µm
0.44	60.7	2.41	100	13.2	100	71.9	100	Span = 1.3
0.49	69.1	2.68	100	14.6	100	80.0	100	Spec. surf. area 16.9911 sq.µ./cc.

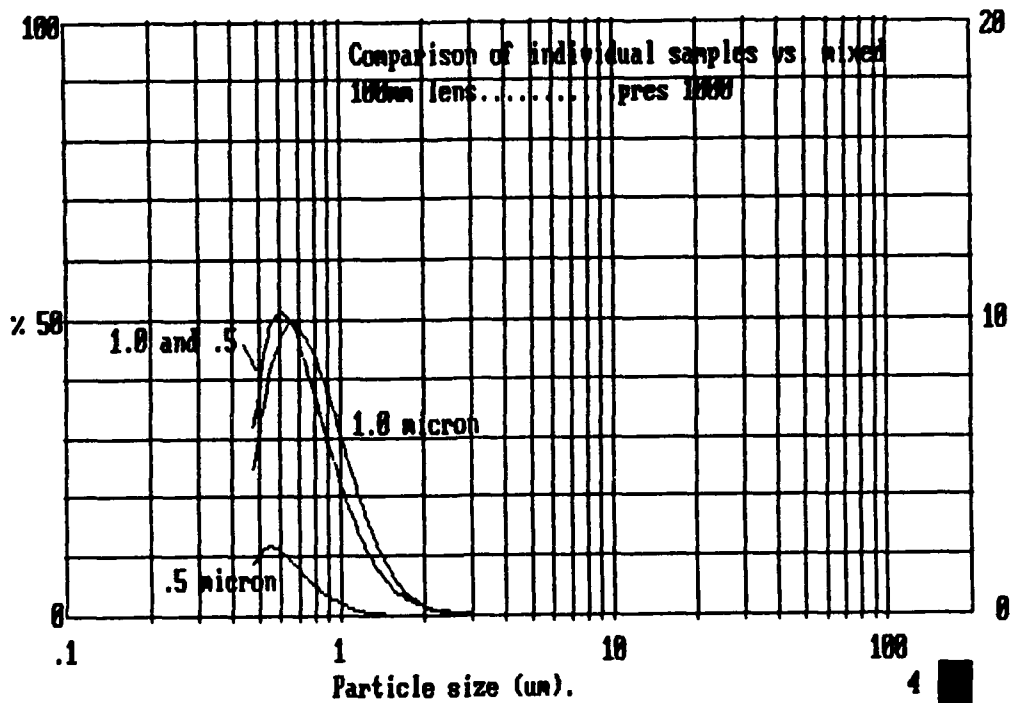
3769 1000 lgu376m

Figure 17a. Mastersizer Validation Results:
0.5 micron spheres



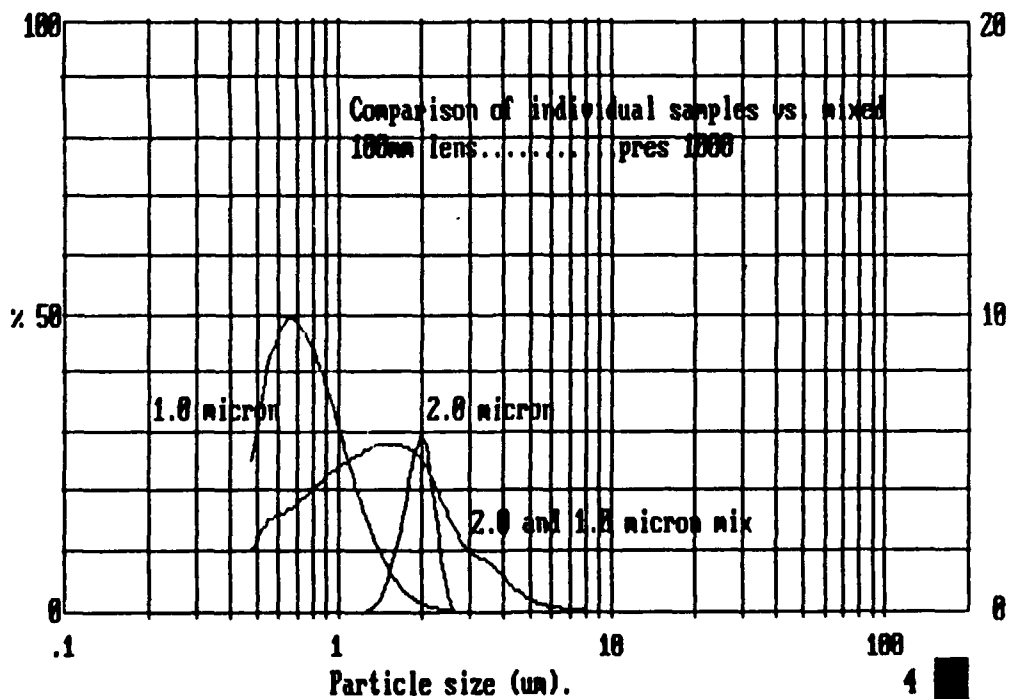
3769 1000 lgu376m

Figure 17b. Mastersizer Validation Plots:
0.5 micron spheres



3769 1000 lgu376m

Figure 17c. Mastersizer Validation Individual and Mixed Samples



3769 1000 lgu376m

Figure 17d. Mastersizer Validation Individual and Mixed samples

LIST OF REFERENCES

1. Netzer, D. W., "Tactical Missile Propulsion - Design and Application", Unpublished Course Notes, Naval Postgraduate School, Monterey, California, April, 1989.
2. TRW Report No. 11709-6003-RO-00, Instruction Manual for Ruby Laser Holographic Illuminator, by R. F. Wuerker, February 1970.
3. Air Force Rocket Propulsion Laboratory Technical Memorandum 78-12, Operation Manual for Lens-Assisted Multipulse Holocamera with Reflected Light Option, by R. F. Wuerker and R. A. Briones, July 1978.
4. Smith, M. J., An Experimental Investigation in the Behavior of Metallized Solid Propellants, Master's Thesis, Naval Postgraduate School, Monterey, California, December, 1988.
5. Butler, A. G., Holographic Investigation of Solid Propellant Combustion, Master's Thesis, Naval Postgraduate School, Monterey, California, December, 1988.
6. Phone Conversation with Mr. Mark Salita, Thiokol Corporation, Brigham City, Utah, 19 November 1989.
7. Phone Conversation with Mr. Jim Thomas, Lawrence Livermore Laboratories, Livermore, California, 4 December 1989.
8. Mastersizer Instruction Manual, Malvern Instruments Ltd., Manual Version IM100, issue 2, August 1988.
9. Paty, R. P., Holographic Particle Sizing in Solid Fuel Ramjets, Master's Thesis, Naval Postgraduate School, Monterey, California, September, 1988.

INITIAL DISTRIBUTION LIST

- | | | |
|----|---|---|
| 1. | Defense Technical Information Center
Cameron Station
Alexandria, Virginia 22304-6145 | 2 |
| 2. | Library, Code 0142
Naval Postgraduate School
Monterey, California 93943-5002 | 2 |
| 3. | Chairman, Code 67
Department of Aeronautics and Astronautics
Naval Postgraduate School
Monterey, California 93943-5000 | 1 |
| 4. | Professor D. W. Netzer, Code 67Nt
Department of Aeronautics and Astronautics
Naval Postgraduate School
Monterey, California 93943-5000 | 2 |
| 5. | Kevin J. Arnold
8446 E. Calatina Dr.
Scottsdale, Arizona 85251 | 2 |